Journal Pre-proof

Probabilistic analysis to correlate seismic data with lava extrusion phases at Merapi volcano (Indonesia)

T. Espinosa-Ortega, A. Budi-Santoso, Sulistiyani, N.-T.-Z. Win, C. Widiwijayanti, F. Costa

Please cite this article as: T. Espinosa-Ortega, A. Budi-Santoso, Sulistiyani, et al., Probabilistic analysis to correlate seismic data with lava extrusion phases at Merapi volcano (Indonesia), *Journal of Volcanology and Geothermal Research* (2021), https://doi.org/10.1016/j.jvolgeores.2022.107537

This is a PDF file of an article that has undergone enhancements after acceptance, such as the addition of a cover page and metadata, and formatting for readability, but it is not yet the definitive version of record. This version will undergo additional copyediting, typesetting and review before it is published in its final form, but we are providing this version to give early visibility of the article. Please note that, during the production process, errors may be discovered which could affect the content, and all legal disclaimers that apply to the journal pertain.

Probabilistic analysis to correlate seismic data with lava extrusion phases at Merapi volcano (Indonesia)

T. Espinosa-Ortega[a], A. Budi-Santoso[b], Sulistiyani[b], N-T-Z. Win[a], C. Widiwijayanti[a], F. Costa[a,c,d]

[a]Earth Observatory of Singapore, Nanyang Technological University, Singapore.

[b]Balai Penyelidkan dan Pengembangan Teknologi Kebancanaan Geologi, Centre for Volcanology and Geological Hazard Mitigation, Geological Agency, Indonesia.

[c]Asian School of the Environment, Nanyang Technological University, Singapore

[d]Institut de Physique du Globe de Paris, Université de Paris, France

Abstract

Volcanoes can produce a range of eruptive behavior even during a single eruption, changing quickly from effusive to explosive style, and the other way around. The changes in eruption phases (e.g. phreatic explosion, magmatic explosion, lava extrusion, etc.) can lead to different volcanic hazards and require timely assessment for the implementation of mitigation measures. Here we explore how to correlate a given eruption phase with changes in the monitoring data using statistical analysis and conditional probabilities. We calculate the success of detection of an eruption phase using a threshold of monitoring data, which includes the uncertainty on the eruption phase dates with a Monte Carlo simulation. We apply the method to dome forming eruptions of Mt. Merapi (Indonesia) and evaluate their time occurrence using an exceptionally long monitoring time series (from 1993 to 2012, over nineteen years) of Multiphase (Hybrid) Seismic Energy. We identify the seismic energy threshold that is associated with the lava extrusion phase with an accuracy of 90 +/- 2%, precision of 73 +/- 2%, specificity of 96 +/- 1 %, and sensitivity of 56 +/- 1%. We further test our method with the recent 2018 eruption (not used in the

thresholds calculations) and we identify the lava extrusion with a precision of 67%, specificity of 70%, and sensitivity of 92%. We also seismically detected the $2018's$ onset of the lava extrusion phase 14 days earlier than the visual observation. Given the link between dome-collapse pyroclastic flows and growth episodes of the lava dome at Merapi, our analysis also allows us to establish that 83% of the most energetic pyroclastic flows occur within the first 3 months after the onset of lava extrusion phase. Our method can be applicable to a range of time series of monitoring data (seismic, deformation, gas) and to other volcanoes that have a significant number of past events.

1. **Introduction**

Understanding the dynamics of volcanic eruptions, their likely eruptive style, and how they evolve through an episode of unrest are among the most important and still challenging problems in volcanology. The physical nature of volcanic systems is highly complex and involves many parameters, which makes it difficult to approach using deterministic models (Sparks, 2003). Thus, assessment of the volcano status and forecasting models commonly rely on statistical methods based on the past eruptive behaviour, including uncertainties and fluctuations inherent to the volcanic system (e.g., Newhall and Hoblitt, 2002; Marzocchi and Zaccarelli, 2006; Selva et al., 2014; Tonini et al., 2016; Bebbington and Lai, 1996; Bebbington and Jenkins, 2019; Pesicek et al., 2021).

The proper assessment of volcano-related hazards depends largely on our ability to identify the monitoring data and patterns associated with a given eruption phase. The success of event detection relies on data quality (e.g. accuracy, completeness, consistency) as well as on the number of times the event has occurred in the past. To use statistical analysis, it is essential to have significant eruptive and monitoring datasets formatted in a consistent manner. The

WOVOdat database of volcanic unrest is one of such standardized resource that allows for the comparison of unrest patterns between eruptions (Newhall et al., 2017; Costa et al., 2019).

The identification of the change of a volcano's normal to an unrest state, and the further progression towards eruption is largely based on the availability of time series monitoring data, including geophysical, geodetical, geochemical, and hydrological signals (e.g. Newhall & Dzurisin, 1988; Shroder & Papale, 2015; Loughlin et al., 2015; Gottsmann, 2019). Analysis of the monitoring data can be used to identify threshold values as the volcano moves from one state to the next (Potter et al., 2015), or to apply auto-regressive models to classify unrest intensity (Carlà et al., 2016).

The recent advancement of satellite remote sensing techniques allows detection of volcanic activities in the form of continuous time series data e.g. thermal, deformation, gas emission (e.g. Coppola et al. (2016); Flower and Carn (2015); Reath et al. (2019)). Challenges to exploiting satellite data include ensuring regular and more frequent acquisitions over active volcanoes and developing tools for automated analysis of the massive volume of imagery for volcano-related signals (Arnold et al. (2017); Poland et al. (2020)). Despite the advantages of satellite remote sensing, these tools strongly depend on the weather conditions, therefore is essential to also correlate other ground-based monitoring data.

The temporal evolution of unrest can be manifested by various types of eruption phases (e.g. phreatic explosion, magmatic explosion, lava extrusion, etc.), which also define the eruption chronology (Costa et al. (2019)). An eruption may consist of many phases (Global Volcanism Program (2013)). Some examples at different volcanoes have been illustrated and described in a chronological manner by Bebbington and Jenkins (2019). Long-duration volcanic eruptions

provide an ideal target for studying temporal evolution of magmatic processes (Bebbington and Jenkins (2019)), the transitions between eruptive style and the underlying processes (Cashman and Sparks (2013); Segall (2013); Watts et al. (2002); Arnold et al. (2017)).

We have developed a method for eruption phase detection using a simple statistical procedure that correlates the eruption phases with the values of monitoring parameters. We calculate the probability to observe an on-going lava extrusion phase at Merapi (Java, Indonesia) using the multiphase seismic energy as the indicator parameter. As there are no accurate dates for the 'beginning' and 'end' of the lava extrusion phases (due to a lack of data or discrepancies between reports) we used Monte Carlo simulations to randomly consider different lava extrusion phase chronologies and calculate their respective conditional probabilities. We assess the efficiency of the detection of lava extrusion phases using different seismic energy thresholds by calculating the accuracy, precision, specificity, and sensitivity (defined in detail in Section 3.2.1). Growing domes tend to collapse and generate pyroclastic density currents, and thus we also explore this relationship and calculate the probably of occurrence with the view of better evaluation of hazards related to dome eruptions.

1.1. Previous works regarding anticipating eruptions of Merapi

Merapi is among the most hazardous volcanoes in Indonesia, and is well-known for its lava extrusion phases that produce dome growth, dome-collapse, and associated hazardous "Merapi-Type" pyroclastic flows (Voight et al., 2000; Newhall et al., 2000; Ratdomopurbo & Poupinet, 2000). The accurate identification and eventual forecasting of lava extrusion phases is thus of great importance to mitigate the impacts of the associated pyroclastic flows (PFs) generated by dome collapse (Calder et al., 2002; Ogburn et al., 2015). Anticipating the evolution of dome

growth is very difficult since lava extrusion dynamics are highly nonlinear (Melnik & Sparks, 1999) and are strongly controlled by the volcano's summit morphology (Walter et al., 2013; Zorn et al., 2019).

Previous analysis of monitoring data of Merapi eruptions include those of Ratdomopurbo and Poupinet (2000), and Young (2007) who used the monitoring geophysical data to compare different eruption phases and assess precursor signals (in hindsight) to gain a better understanding of the driving mechanisms of dome collapse events at Merapi. Moreover, the Center for Volcanology and Geological Hazards Mitigation (CVGHM) of Indonesia developed a fuzzy inference system using a local instance of the WOVOdat system at Merapi observatory, and analysed multi-parameter monitoring data (e.g. seismic counts, EDM-distance changes) of five past unrest events (Budi-Santoso et al., 2018a). The indicators obtained were then used as the input of a model which yielded two output variables: the alert level change and eruptive style (effusive or explosive).

An important aspect to be considered for detecting Merapi's dome eruptions is the accurate identification of the onset and duration of the lava extrusion phases. This is not straightforward due to a variety of reasons including the limited access and visibility of the active lava dome, the slow extrusion rate and endogenous regime of lava dome growth (Voight et al., 2000b, Young, 2007), the numerous and intermittent explosions (Pallister et al., 2013; Budi-Santoso et al., 2013), and the occurrence of multiple vent extrusions sites (Voight et al. 2000a, Ratdomopurbo et al., 2013). Proper identification of onset and evolution of lava extrusion phases is however necessary to anticipate their potential hazards including the generation of PFs caused by dome collapse due to gravitational instability or heavy rain (Carn et al., 2004; Hale, 2008; Walter et al.,

2013), dome fractures that suddenly release the pressure in the lava conduit (Watts et al., 2002; Walter et al., 2015), or/and hydrothermal alteration of the dome permeability (Heap et al., 2019). In most cases the dome-forming eruptions are also associated to explosive phases (Newhall & Melson, 1983; Ogburn et al., 2015; Calder et al., 2015).

Another important aspect for detecting lava extrusion phases is to be able to correlate them with some type of monitoring data. Hybrid volcanic earthquakes, characterized by high-frequency onsets and with low-frequency tail seismic signals (e.g. Power et al., 1994; McNutt, 2005), occur during shallow brittle rock failure that may relate to dome building processes (Wassermann, 2012 Harrington & Brodsky, 2007; White & McCausland 2016). In general, these earthquakes are shallow and thus preserve most of their high-frequency energy (Neuberg et al., 1998). The seismic energy has been used to characterize the size, generation and transport of PFs at Merapi (Iguchi et. al., 2019) and other volcanoes (e.g.Yamasato, 1997,; De Angelis et al., 2007). Brodscholl et al., 2000 used seismic broadband data to characterize the 22 November 1994 sequential lava dome collapse PF at Merapi, where the seismic signal exhibits a linear relation between source volume and recorded seismic-amplitude envelope area. PF and Rockfall (RF) seismic amplitude-duration data were used as proxies to estimate collapsed lava dome volume of Merapi (Young, 2007).

At the Merapi observatory, hybrid volcanic earthquakes are classified as multiphase (MP) earthquakes Fig. 1 (Budi-Santoso et al., 2013). We use Merapi's Seismic Energy time series of MP and PF earthquakes covering a period of almost 20 years from 4 February 1993 to 31 December 2012; this period of time includes 7 lava extrusion phases (described in section 2.2). The time series data, the eruption chronology, and the tools are also available and freely accessible in WOVOdat (www.wovodat.org).
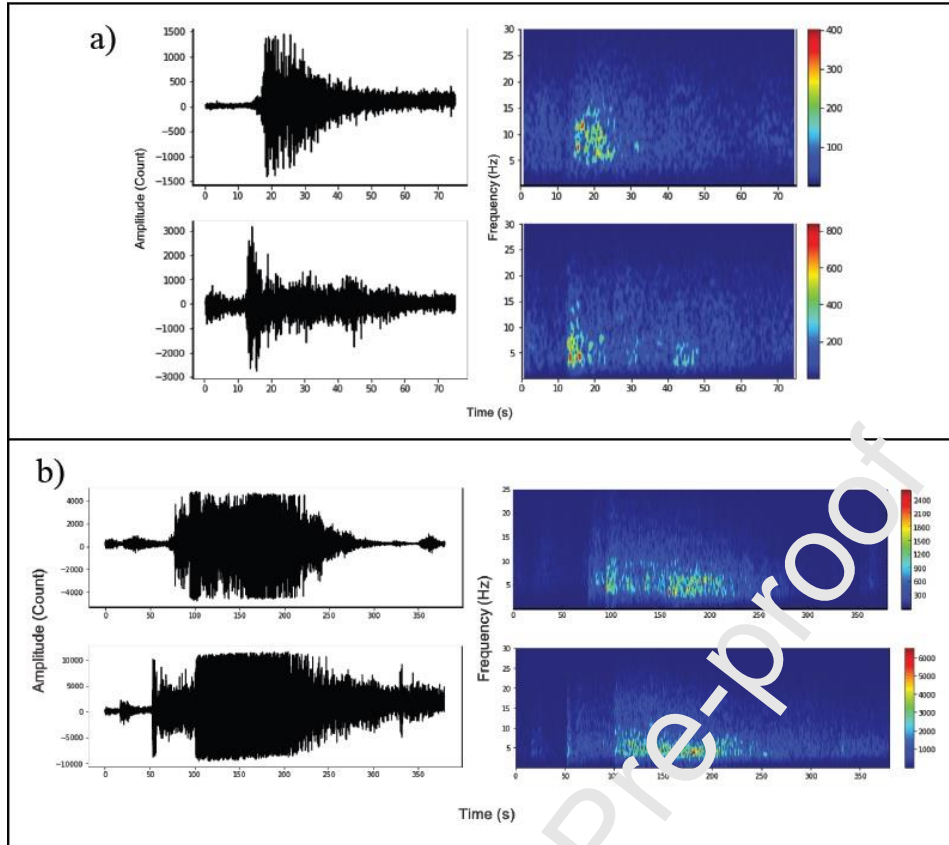
Figure 1 Examples of the multiphase (MP) and pyroclastic flow (PF) seismic signals recorded at Merapi. The waveform (left panel) and spectrogram of the waveform (right panel) are shown. A) MP earthquakes from 14 June 2006 and 26 October 2010 ; b) PF earthquakes from 14 June 2006 and 26 October 2010.

2. Seismic and historical eruption phases

2.1. Seismic Data

The modern seismic monitoring network at Merapi (Fig.2) was operational in 1982 (Ratdomopurbo & Poupinet, 2000). It consisted of 7 stations equipped with short-period seismometers (Mark Product L4C); the location of the 4 main seismic stations used in this study are shown in Fig 2. The Pusunglondon (PUS) station is 0.9 km from the crater, and is the main reference station used to routinely monitor Merapi seismic activity including drum plot manual reading to determine earthquake type, daily earthquake counts, first arrival phase and calculation

of seismic energy (Budi-Santoso et al., 2013). The Klatakan (KLA), Deles (DEL) and Plawangan

(PLA) seismic stations are located within a radius of 5.3 km from the crater and are typically

used as the secondary reference stations to validate PUS readings. Most of the instruments of

these stations were replaced after the PF of the 2010 eruption destroyed them, first the KLA

station on 3 November and later the PUS and DEL stations on 4 November (Budi-Santoso et al.,

2013); later the seismic activity was registered only using the PLA station. Moreover, the large

amplitude of the low-frequency (LF) seismicity during 2010 saturated the other signals, and thus

it displays unusually low (below10 MJ) MP energy values. The metadata with instrument and

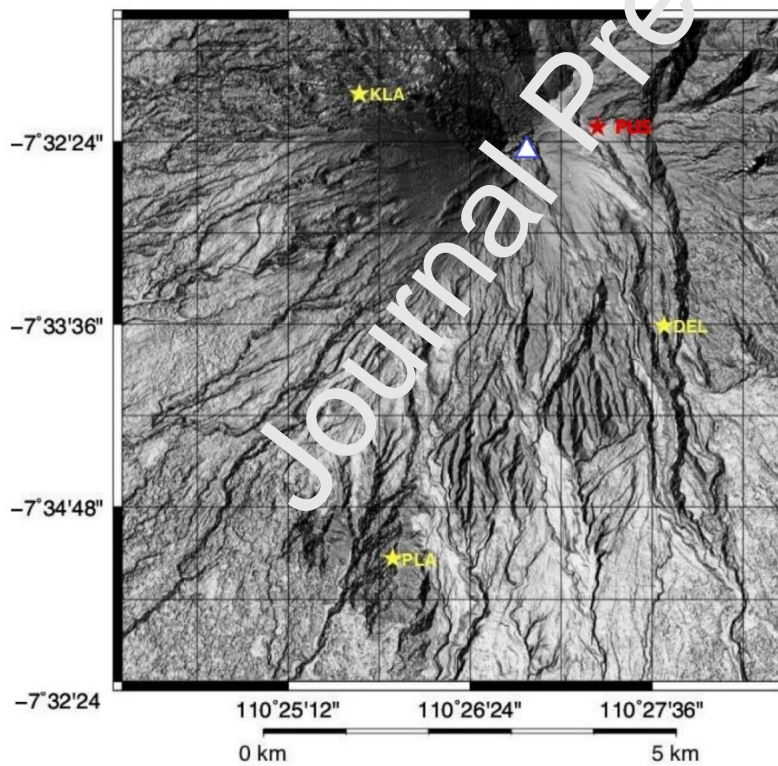operational details is described in Tables 1 and 2.

Figure 2. Location of the four main seismic stations at Merapi network, composed of short-period and broadband stations operated between 1994 and 2018, overlaid on top of Merapi shaded relief map based on DEM from Gerstenecker et al. (2005) combined with 2012 Lidar and 2018 drone surveys performed by CVGHM. PUS seismic station, location marked in red star, is the primary reference station for the measurement of MP and PF seismic energy. KLA, DEL and PLA seismic stations marked by yellow stars are the seismic stations referred to for the determination of earthquake type.

Start Date	End Date	Seismometer	Natural Frequency (Hz)	Components	Damping factor
1982	4th November 2010	Mark L4C3D	1	3	0.8
April, 2011	December, 2016	Mark L22	2	1	0.7
December, 2016	now	Sercel L4C	1	1	0.8

Table 1. Operational timeline of seismic instruments at PUS station between 1982 and present, illustrating data continuity and consistency.

Seismic Stations	Seismic Instruments	Start Time	End Time	Latitude (^{o}S)	Longitude (^{o}E)	Elevation (m)
Pusunglondon (PUS)	Mark Product L4C	1982	4 November 2010	-7.538359	110.454016	2625
Deles (DEL)	Mark Product L4C	1982	2010	-7.561951	110.462504	1918
Klatakan (KLA)	Mark Product L4C	1982	2010	-7.534735	110.42784	1487

	Mark Product L4C	1982	2011	-7.584137	110.432253	1276
Plawangan (PLA)						
Pusunglondon_2010 (PUS_2010)	Mark Product L22	22 November 2010	30 November16	-7.538359	110.454016	2625

Table 2. Metadata of Merapi's seismic stations used in this study. PUS is the main station and DEL, KLA, and PLA as supplementary stations that are used to monitor Merapi seismic activities, which include earthquake classification, daily counts, hypocenter relocation and quantification of seismic energy. All sensors are analog type.

The CVGHM has kept a consistent daily record of Merapi's seismic activity since 1982. The frequency, duration, and amplitude of the seismic waves have been used to manually classify earthquake types, which in turn have been associated with different processes (Minakami, 1960; Shimozuru, et al., 1969; Ratdomopurbo & Poupinet, 2000; McNutt & Roman, 2015). Volcano tectonic (VT) earthquakes are associated with brittle failure of rocks due to the migration of magma towards surface, they can be either deep (VTA), between 2.5-5 km, or shallow (VTB), less than 1.5 km below summit. There is a gap in the hypocenter depth between 1.5-2.5 km; this aseismic zone has been associated with the location of a shallow magma pocket (Nandaka et al. (2019)) and the presence of a more ductile zone in between brittle layers (Ratdomopurbo and Poupinet (2000)). LF events are associated to fluid resonance and degassing of rising magma (Hidayat, et al., 2002). RF and PF seismic events are related to the instability of the dome, outflow of lava, and dome collapse phenomena. Finally, the so-called MP events are associated with magma flow in the upper conduit and a shallow process that occurs during dome formation (Wassermann, 2012); Budi-Santoso et al., 2013; Jousset et al., 2013). These earthquakes are

similar to the hybrid earthquake signals at other volcanoes (McNutt 2005; Zobin 2012) and are characterized by emergent onsets, with a range of frequency contents between 0.2 and 20 Hz (Jousset et al., 2013), but with a dominant frequency between 4 to 8 Hz (Fig. 1a.). For a given amplitude, the duration of a MP event can be twice that of VT earthquakes; they occur at shallow depth, and are sometimes also correlated with summit deformation due shallow magma intrusion (Aisyah et al., 2018; Ratdomopurbo and Poupinet, 2000; Budi-Santoso et al., 2013; Beauducel et al., 2000, 2006).

Hybrid or long-period, VT and RF earthquakes have been observed during the growth and collapse of the lava dome at many volcanoes (Zobin, 2012) such as Soufrière Hills (Miller et al., 1998; Gardner and White, 2002; De Angelis et al., 2007; Neuberg, 2000; Luckett et al., 2008), Redoubt (Lahr et al., 1994; Lowenstern, 2016; Bu'l and Buurman, 2013; Costa et al., 2019), Unzen (Lamb et al., 2015; Nakada et al., 1999; Umakoshi et al., 2008), St. Helens (Harrington and Brodsky, 2007), Colima (Arámbula-Mendoza et al., 2018; Zobin et al., 2014), Sinabung (McCausland et al., 2019), Santiaguito (Johnson et al., 2008) and Pinatubo (Hoblitt et al., 1996; Newhall et al., 2017). VT earthquakes, which are dominated by high frequencies, have been linked to magma breaking paths to the surface and the associated stresses (Roman et al., 2006). Swarms of hybrid earthquakes, events with a similar high frequency initial phase to the VT events but with an additional lower frequency monochromatic phase or long period coda (Power et al. (1994); McNutt (2005)), replaced VT earthquakes as the most common event type during dome growth (Miller et al. (1998)). On the other hand, rockfall signals are thought to be caused by violent degassing at the surface of the dome that triggers a nearby rockfall, while LP earthquakes are interpreted as pressurization in the conduit (Luckett et al. (2002, 2008)).

We first did a preliminary analysis of the different earthquake types that may be related to lava extrusion. At Merapi, VT and LF events are known to precede lava extrusion (Nandaka et al., 2019; Iguchi et al., 2019), but the time delay between when they appear and the onset of lava extrusion phase is highly variable, and in some cases, they are absent. VT and LF earthquakes have also been observed during lava extrusion phases, although their appearance is infrequent. In particular, in 1996 several LF seismic events were reported (Nandaka et al. (2019)) at the same time that dome formation was observed (Voight et al. (2000a); Young (2007)). Similarly, at the end of 2000 a new lava extrusion phase started (Young (2007)) during a very active period of VT earthquakes (Nandaka et al. (2019)).The RF events are also present and increase during the lava extrusion phases, but they persist even after the lava extrusion stops, which is likely due to gravitational slope instabilities of the dome (Voight, et al., 2000). The MP events are the most directly connected to magma flow in the upper conduit and to lava extrusion/dome growth (Budi-Santoso et al., 2013; Ratdomopurbo & Poupinet, 2000; Wassermann, 2012).

Here we use the seismic energy associated with MP earthquakes (Fig. 3) as calculated by the CVGHM using the Gutenberg-Richter equation: $log\,(E) = 11.8 + 1.5M$, where M is the magnitude (Gutenberg & Richter, 1956) and E is energy in ergs. Magnitude calculation follows the formulation of Richter for local earthquakes recorded by Wood-Anderson type stations, $M = Log(A_r) + Log(A_0)$, where M is the local magnitude, A_r is the amplitude of Wood Anderson's seismograph shift in mm, and $Log(A_0)$ is a constant that is proportional to the epicenter distance. In the case of Merapi, the epicenter distance is within about 5 km radius, the $Log(A_0)$ = -1.4. Moreover, $A_r = 2800A/(G * Cg)$, where A is the amplitude recorded by the seismograph, G is the magnification of the seismograph, and Cg is the soil amplification factor. G and Cg values for PUS stations are 800 and 0.9, respectively. In addition, the seismic energy

related to PFs is also computed. PFs generated by dome collapse produce RF-type signals but with more impulsive onset of long duration (up to tens of minutes) and large enough amplitudes to be recorded at the farthest stations in the network (Fig. 2). The PF energy was obtained by multiplying the maximum amplitude and duration of the seismic wave by which we obtained an arbitrary unit (a. u.) of its energy equivalent. Here we analyzed MP and PF seismic energy.

2.2 Lava extrusion phases

We studied the period between 4 February 1993 and 31 December 2012, during which time Merapi had 4 eruptions (Table 3) and a range of different eruption styles including: lava extrusion, magmatic explosions and phreatic explosions (Voight et al. (2000a); Ratdomopurbo and Poupinet (2000); Ratdomopurbo et al. (2013)). Here we focus on the 7 lava extrusion phases that occurred in this period (Table 4). Six of these consisted of long periods of slow lava-dome growth, lasting weeks to months; whereas the 2010 lava extrusion phase involved intermittent dome growth and explosions. The range of dates selected include the full duration of the 7 lava extrusion phases and the pauses in between.

The eruptive phenomena of Merapi between 1994 and 2006 include near-continuous, mostly endogenous basaltic-andesite lava-dome growth that filled the crater floor and piled on top of previous lava domes that create structural discontinuity at the summit edifice (Voight et al., 2000; Ratdomopurbo and Poupinet, 2000; Ratdomopurbo et al., 2013). Between the seven lava dome extrusion phases (Table 4), there are periods of repose or with minimal extrusion, which we categorized as periods of no lava extrusion. The periods of 'unrest' before the reported onsets of lava extrusion varied greatly for different events, therefore we arbitrarily categorized as precursor activity the 15 days preceding the onset (details discussed in section 3.1).

The lava extrusion phases are typically followed by small to moderate size rockfalls, sometimes accompanied by vulcanian explosions (as in 1997 and 1998; Nandaka et al., 2019), and in the later stages of the phase, the lava dome becomes unstable and produces dome collapse PFs. In addition, small phreatic explosions are also common, as happened between 2012 to 2014 following the 2010 eruption (Metaxian et al., 2020). More recently, after four years of quiescence, renewed phreatic explosions occurred in May 2018 and were followed by effusive activity. The new lava dome extrusion was observed on 11 August 2018 and slow extrusion continued until September 2019 (Kelfoun et al., 2021).

Eruption	Onset	End
1	20 Jan 1992	19 Oct 2002 *
2	16 Mar 2006	9 Aug 2007*
3	26 Oct 2010	15 Jul 2012
4	11 May 2018	21 Jun 2020

Table 3. Eruption timeline. Confirmed Eruptions of Merapi. *uncertain dates. Data from Global Volcanism Program (2013)

Phase	Onset	End	Lava Extrusion rates	References
1	1-28 Feb 1994 *	22 Nov 1994	0.07-0.19 $m3/s$ (Feb-Aug 1994)	Voight et al., 2000; Young, 2007 ; Ratdomopurbo et al., 2013
2	9 Aug-30 Sep 1996*	13-31 Jan 1997*	0.27-2 $m3 / s$ (Aug 1996-Jan	Voight et al., 2000; Young, 2007; Iguchi et al., 2019

			1997)	
3	**31 May-9 Jun 1997***	**20-30 Sept 1997***	-	Young, 2007 Fig.3-13; Nandaka et al., 2019
4	30 Jun 1998	**1-10 Jan 1999***	0.5 $m3/s$ (Jun-Jul 1998)	Voight et al., 2000a; Young, 2007
5	31 Oct 2000	**1-28 Feb 2001***	0.8-0.5 $m3/s$ (Jan-Feb 2001)	Young, 2007
6	10 Apr 2006	**15 Sep-31 Oct 2006***	1-3.3 $m3/s$ (Apr-Jun 2006)	Young, 2007; Budi-Santoso et al., 2008; Ratdomopurbo et al., 2013; Walter et al., 2013; Carr, et al., 2016
7	**21-28 Oct 2010***	08 Nov 2010	25-35 $m3/s$ (Nov 2010)	Surono et al., 2012; Cronin et al., 2013; Pallister et al. (2013)

Table 4. Time-line of the lava extrusion phases, the dates with asterisk (*) are the periods when the onset/end date of activity are not precisely known. We also show the lava extrusion rates for some specific dates.

The extrusion rates vary greatly between and within lava extrusion phases (Table 4). In 1994 the lava extrusion rate varied from 0.07 m^3/s in the early lava extrusion phase to 0.19 m^3/s in August, and it was followed by a large dome collapse on 22 November (Voight et al., 2000a; Ratdomopurbo et al., 2006; Young, 2007). The 1996 lava extrusion phase was marked by rapid dome growth with rates that varied between 0.27-2 m^3/s, which culminated in a heightened

extrusion rate of 2 m^3/s on 14 January 1997, and was followed by a vulcanian explosion on 17 January 1997. Based on the dome volume between June and July 1998, the extrusion rate was ~0.5 m^3/s (Voight et al., 2000b; Young, 2007). After 15 months of repose, in mid-January 2001 the extrusion rate reached ~0.8 m^3/s then decreased by mid-February 2001, until the extrusion waned (Ratdomopurbo et al, 2013). In 2006 the extrusion rate ranged from 1 m^3/s to 3.3 m^3/s (Ratdomopurbo et. al. 2013), whereas in 2010 the lava extrusion was 25 m^3/s on 1 November, and culminated on 6 November with a rate of 35 m^3/s (Surono et.al 2012; Pallister et al., 2013). As there are no precise lava extrusion rates for the entire investigated period, we do not directly use the extrusion rates in our analysis, but rather use them to complete the lava extrusion phase chronology (Table 4). Thus, we considered dates when the lava extrusion was reported even if there are no estimations of the extrusion rate.

Due to the complexity of the dome formation and surveillance, the dates of when the lava extrusion occurred are not precisely known (Table 4). Where the onsets/end of lava extrusion do not have exact dates and are referred as "early" or "late" by the data sources, we used the first 10 or the last 10 days of the month, respectively, as an estimate to define the uncertainty windows, respectively. The uncertainty in these dates is taken into account in the probability distribution of the monitoring time series. A detailed chronology of Merapi unrest between 1994 and 2019 is reported in the Supplementary Material.
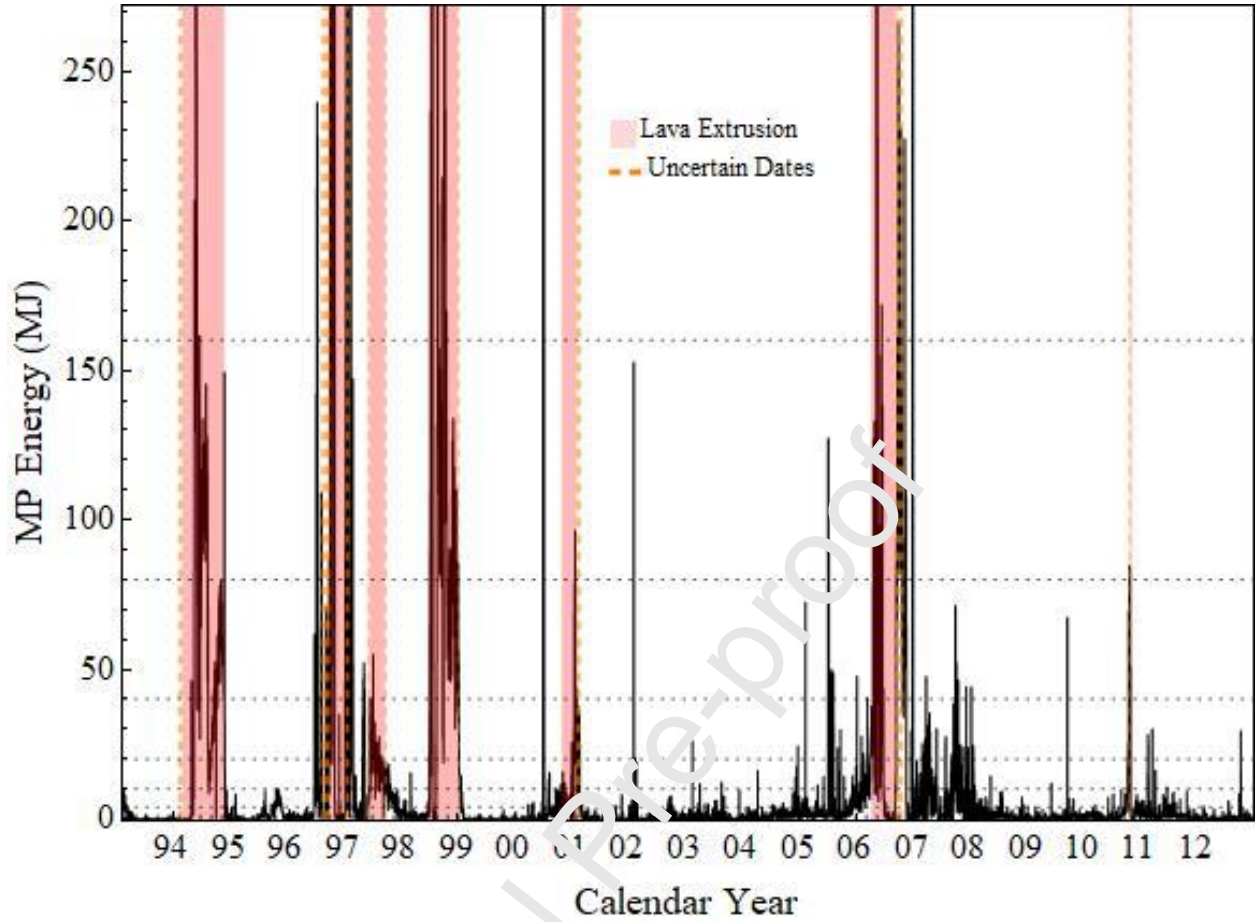
Figure 3. Merapi daily multiphase (MP) energy (in black) between 4 February1993 to 31 December 2012. The light-red vertical bands mark the lava extrusion phases, the uncertain dates are shown by vertical the dashed red lines. The horizontal dashed lines are for reference and indicate energy intervals as used in Section 3.

3. Methodology and results

In this section we present an approach to calculate the conditional probabilities to detect an on-going eruptive phase given the measured values of the monitoring data of the daily seismic multiphase energy (MPE). First, we explain the use of Monte Carlo simulations to account for the uncertainties in the lava extrusion start and end dates (Table 4). Later, we calculate the probability to observe a lava extrusion phase given the range of MPE, and compute how these

probabilities have evolved over the years at Merapi. Finally, we evaluate how the MPE thresholds calculated using data from 1993-2012 could be used to detect the lava extrusion phases of 2018.

3.1 Monte Carlo simulations to account for uncertainties in the lava extrusion phases time-line

To classify the time series data during an eruption phase we need to know its exact 'onset' and 'end' dates, but these are not well known or have been inconsistently reported. From 4 February 1993 to 12 December 2012 Merapi experienced 7 lava extrusions phases (Fig.3), but their onset/end are only known within a few days to months (Table 4). Considering these uncertainty windows, the number of possible combinations of the onsets/end dates for all lava extrusion phases is of the order of 10^{11} cases (see supplementary material for details). To account for this large number of combinations, we used a Monte Carlo approach where we randomly selected the onset/end dates within the uncertainty windows and calculated the probabilities to observe a lava extrusion as a function of the daily MPE, then repeated the process for another random set of dates 10^4 times. The uncertainty in these dates is reflected in the probabilities as the standard deviation of the stochastic simulations.

3.2 Analysis of the time series

Using the randomly generated sets of onset/end dates of the 7 lava extrusion phases in Table 4, we classified the seismic monitoring time series from 1993-2012 into three different periods:

I. Active period: These are the daily MPE values of the days during the lava extrusion phase even if these days are not consecutive or occur simultaneously with other eruptive phases.

II.   <u>Precursory period</u>: These are the daily MPE values of the days that precede the onsets of the lava extrusion phase and therefore can capture the transition of activity in the volcano. Here we arbitrarily choose 15 days prior to every onset.

III.   <u>Non-active period</u>: These are the daily MPE values of the days that are neither the periods of precursors nor of the active period. These are not necessarily days without volcanic activity, as they may include other types of eruptive phases different from the lava extrusion phase that we focus upon here.

We calculate both, the probability $P(k|i)$ to have a daily MPE within the interval k, for each period (i = I, II and III) and also the probability $P(i|k)$ to observe each period (i=I, II, III) given a daily value of the MPE:

(1) $\quad P(k|i) = \frac{f_i(k)}{\sum_k f_i(k)} = \frac{f_i(k)}{Total\ days\ in\ period\ i}$

(2) $\quad P(i|k) = \frac{f_i(k)}{f_I(k) + f_{II}(k) + f_{III}(k)} = \frac{f_i(k)}{Total\ days\ with\ MPE\ \epsilon\ k}$,

where $f_i(k)$ is the number of days that a period i had a daily MPE value within a given interval k. The k intervals were arbitrarily divided by the energies: 0, 1, 4, 10, 20, 50, 100, 200, 400, >400 in MJ, meaning the bin-width intervals k are [0,1) MJ, [1,4) MJ, and so on (Fig.4). The conditional probabilities Eqs. (1, 2) are related to each other according to the Bayes theorem, $P(i|k) = \big(P(k|i)P(i)\big)\big(P(k)\big)^{-1}$, where *P(i)=(Total days in period i)/(Total days)*, is the unconditional probability to have a period i, and *P(k)= (Total days with MPE ϵ k)/(Total days)*, is the unconditional probability to have a day with daily MPE values within the interval k.

The probabilities Eqs.(1, 2), give us complementary information. $P(I|k)$ is the fraction of days with MPE values within the interval k when the active period (lava extrusion phase) occurred,

whereas $P(k|I)$ is the fraction of days in the active period that had MPE within the interval k. The probability distribution $P(k|i)$ allows us to determine the dominant seismic energy for each of the three periods. We found that the probability distribution for the days within the active period (i = I) has a peak at the MPE interval [40,80) MJ (Fig 4). The maximum value of the MPE interval is between 20 and 160 MJ, and does not vary significantly by including more lava extrusion phases (Fig 4a), which suggests that the use of these energy intervals is a robust indicator of the lava extrusion phase. Moreover, we found that the probability distributions of each period have a maximum probability at different energy intervals (Fig. 4b).
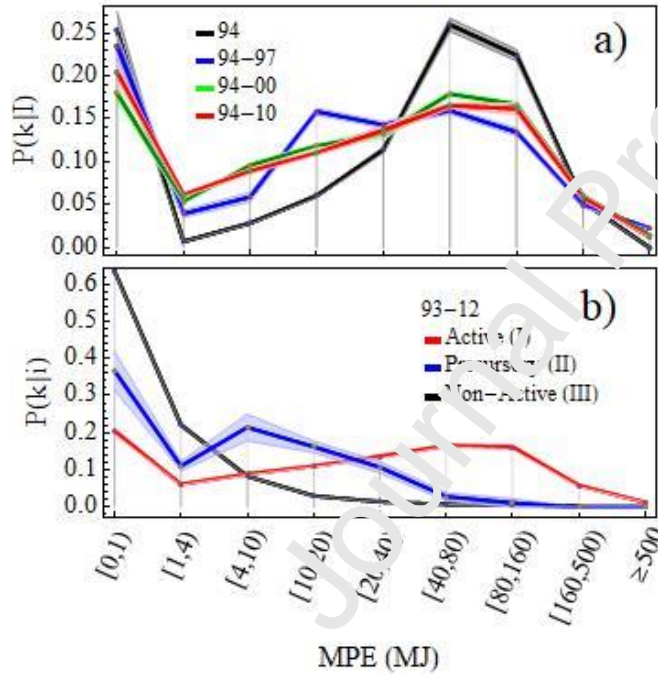
Figure 4. a) Change of the probability $P(k|I)$ (Eq.(1) with i=I)) for MPE during the active period. The colors of each line indicate the lava extrusion phase year(s) that were included in the calculation, and vary from the 1994 only (black line) to all lava extrusion phases from 1994 until 2010 (red line). b) Probability (Eq. (1)) to have a given MPE during each period (active, precursory, or non-active) from 1993-2012 . The solid lines are the mean of the iterations and the shaded areas the standard deviation of the stochastic simulations that are related to the uncertainty of the lava extrusion phase time-line (section 3.1). Please note that lines in the upper panel are associated with the year that the active period occurred, whereas the lower panel includes also the precursory and non-active periods.

We also found that the probability $P(I|k)$ to observe an active period (or in other words, the probability to observe an on-going lava extrusion phase) is <0.1 for low values of MPE, but it quickly increases to about 0.8 at the interval $[40,80)$ and remains high for higher MPE values (Fig.5). The probability to observe a non-active period $P(III|k)$ is almost a mirror image of the active period since it is approximately $1 - P(I|k)$. There is a cross-over of probabilities of the two periods between the MPE intervals of $[10,20)$ and $[20,40)$. The value of 20 MJ is between the two intervals, and can be used to define a so-called *threshold* of MPE. This threshold marks where the probability to observe a lava extrusion phase is higher than no-lava extrusion, and could be used as a critical indicator for decision making (see section below; e.g. Potter et. al., 2015). The probability for the precursory period ($i=I$) is mainly < 0.1 for all energy intervals because the total number of precursor days is much smaller than those of the two other periods given that we have defined it to be 15 days. The choice of the number of days classified as precursor doesn't affect the probability to observe an active phase, since for each stochastic simulation, the number of days in the active period (I) is fixed. Varying the length of the days defined as precursors would only move some days from the precursory period (II) to the non-active period (III) or vice versa. The probabilities shown in Figs. 4,5 were calculated using 7270 days (from 4 February 1993 to12 December 2012) and 10^4 random scenarios.
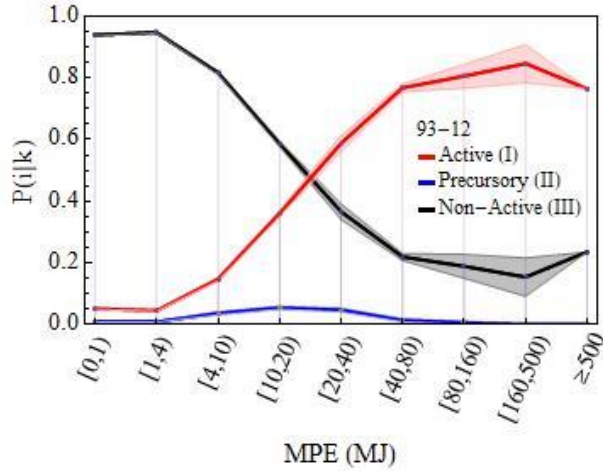
Figure 5. Probability (Eq. (2)) to observe an active period (in red), a precursory period (in blue, or a non-active period (in black), as a function of the MPE, from 1993-2012. The light shaded area around the lines show the uncertainties due to the inaccuracy on the timeline of the lava extrusion phase, and are the standard deviation of the stochastic simulations.

We also calculated whether the probability to observe an on-going lava extrusion phase as a function of the MPE intervals changed over time by accumulating the data progressively, starting from 1993-1994 until 1993-2012 (Fig 6). We found that the probability to detect a lava extrusion phase with ($P(I|k)$ =0.5) shifts to higher MPE through time, starting at MPE below 8 MJ for the event in 1994, up to ~20 MJ when all the phases are included. For instance, from $1993 - 1995$ a daily MPE between $20 - 40$ MJ indicated an on-going lava extrusion with a probability $> 90\%$, whereas from $1993-2005$ the same energy values indicated an on-going lava extrusion with a probability of 70%, and this value further drops to 60% from $1993-2012$. The exact reasons for the changes in probability in specific times are unclear but they could be associated with the state of the volcanic conduit. For example, in an open conduit brittle fracture is not necessary for the lava to extrude and consequently one can expect lower MPE values. In contrast, in plugged conduits the lava extrusion requires brittle fracture and therefore one would expect higher MPE values.

If the lava extrusion phases are analyzed independently, it is not possible to track the threshold evolution, as the lack of significant data for the short duration of some phases (such as 2001 and 2010) create large fluctuations (see supplementary material section-4).
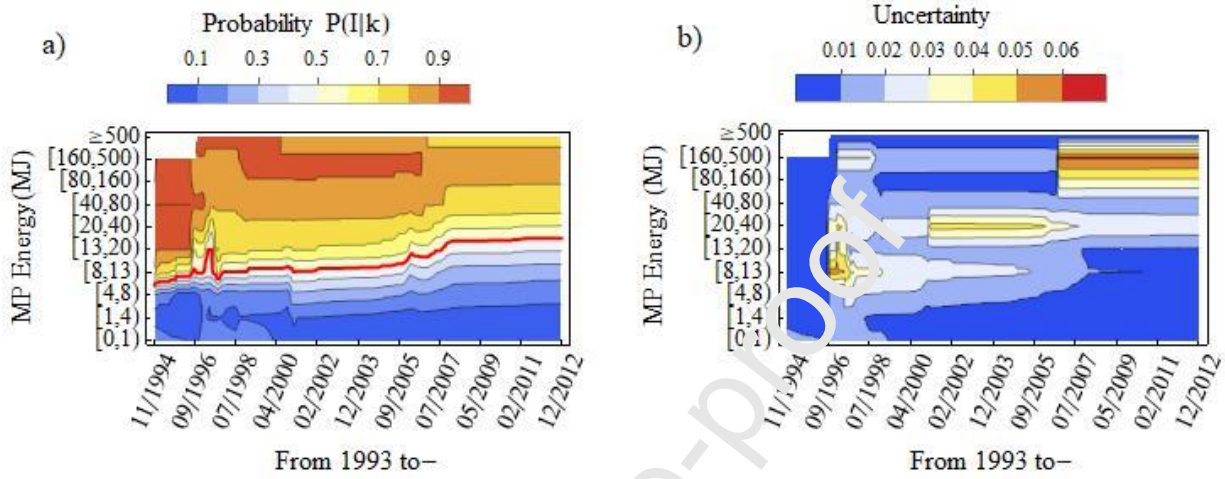

Figure 6. a) $P(I|k)$, Probability to observe an on-going lava extrusion phase as a function of the daily MPE (vertical-axis), and as a function of the data accumulated from 1993 till the date indicated in the horizontal-axis. The thick red line indicates a probability of 0.5. b) Uncertainty (1-standard deviation) related to the poor knowledge of the start and end eruptions data obtained using 1000 simulations for each date in the horizontal-axis.

3.2.1 The use of thresholds for calculating probabilities of lava extrusion

Our analysis of the relationship between seismic energy changes and lava extrusion phases suggests to us that a useful manner to relate the two is using a threshold of MPE values. In other words, it is possible to calculate the probability to detect a lava extrusion phase when the daily MPE is larger than a given value (i.e. a threshold, E) rather than a specific interval of MPE values. The conditional probabilities for the different periods are:

(3) $P(\geq E|i) = \dfrac{f_i(\geq E)}{Total\ days\ in\ period\ i}$,

(4) $\qquad P(i| \geq E) = \frac{f_i(\geq E)}{Total\ days\ with\ MPE \geq E}$,

Where $f_i(\geq E)$ is the number of days that the period i (i=I for active period, etc.), had a MPE $\geq E$. Eqs. (3,4) are similar to Eqs.(1,2), but instead of using MPE within energy intervals, we use MP energies above a threshold. Thus, $f_i(\geq E)$ is equal to the summation over of all the intervals k with MPE $\geq E$, i.e., $f_i(\geq E) = \sum_k f_i(k)$; therefore $P(\geq E|i) = \sum_k P(k|i)$, but, $P(i| \geq E) \neq \sum_k P(i|k)$, as the denominators in Eq. (2) and Eq.(4) are different.

In this section we focus solely on the probability to detect a lava extrusion phase, therefore we reduce the 3 group classification of the previous section, to just two: 'days with lava extrusion' and 'with no lava extrusion' (we merged the precursory (II) and non-active (III) periods into a no-lava extrusion period). The conditional probabilities to detect a lava extrusion phase when the MPE is above an energy threshold can be expressed in terms of the accuracy, precision, sensitivity, and specificity, (Fawcett, 2006) defined as (Table 5):

	Reported Event	
	Lava Extrusion	No Lava Extrusion
Test positive (weekly MPE $\geq$ E)	TP $=f_I(\geq E)$	FP $=f_{II}(\geq E) + f_{III}(\geq E)$
Test negative (weekly MPE $<$ E)	FN$=f_I(< E)$	TN$=f_{II}(< E) + f_{III}(< E)$

Figure 3. TP= True Positive = number of days with lava extrusion with weekly MPE≥E; FP= False Positive= number of days with no lava extrusion with weekly MPE≥E; FN= False Negative=number of days with lava extrusion with weekly MPE<E; TN=True Negative= number of days with no lava extrusion with weekly MPE<E. E is the threshold value of MPE.

(5) $\qquad Precision = \frac{TP}{TP+FP} = \frac{f_I(\geq E)}{Total\ days\ with\ MPE \geq E} = P(I| \geq E)$,

(6) $\qquad Sensitivity = \frac{TP}{TP+FN} = \frac{f_I(\geq E)}{Total\ days\ with\ lava\ extrusion} = P(\geq E|I)$.

(7) $\qquad Specificity = \frac{TN}{TN+FP} = \frac{f_{II}(<E)+f_{III}(<E)}{Total\ days\ with\ no\ lava\ extrusion}$

(8) $Accuracy = \frac{TP+TN}{TP+TN+FN+FP} = \frac{f_I(\geq E)+f_{II}(<E)+f_{III}(<E)}{Total\ days}$.

The precision is the fraction of days with MPE$\geq E$ when lava extrusion phase occurred (positive predictive value); the sensitivity is the fraction days in the lava extrusion phase that had MPE above the threshold (true positive rate); the specificity is the fraction of days that were correctly classified as negatives (true negative rate); finally the accuracy describes the fraction of days that our tests (Table 5) were correct.

Moving average. We evaluated the probabilities with Eqs (5-8), using the daily MPE and also with the average of the MPE from previous days. We found that using a moving average (as done in other studies of time series of monitoring data: e.g. moving window analysis rather than daily; Jaquet et. al., 2006, Alvarez-Ramirez et. al., 2009), improves the precision and sensitivity, as it minimizes the effect of large fluctuations of MPE that appear in consecutive days and it preserves the overall trend in seismic activity.

We found that the optimal size of the time window is 7 days, as explained in the supplementary material. In this manner, the frequencies $f_i(\geq E)$ are equal to the number of days that the period i, had a weekly moving average of MPE $\geq E$ and the denominator of Eq.(5) is equal to the "*Total days with a weekly moving average of MPE$\geq E$*".
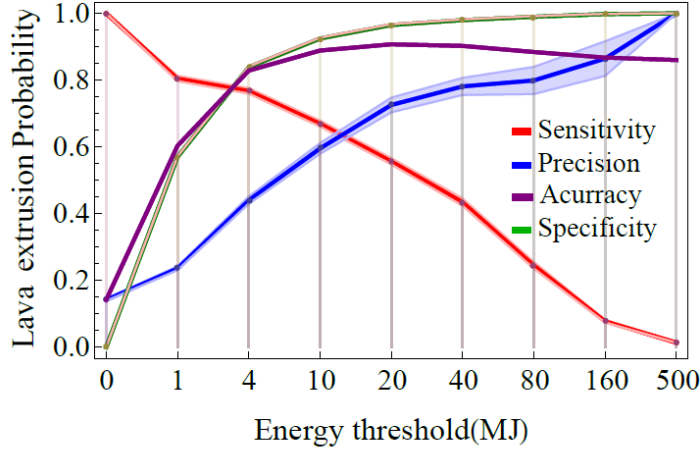
Figure 7. Conditional probabilities to detect a lava extrusion phase using a moving average of MPE of the past 7 days (e.g. weekly average) calculated with Eqs(5-8). Notice the x-axis scale is not linear. Probabilities calculated using 7270 days and 10^4 random scenarios, the solid lines represent the mean of the iterations and the shaded area around the solid lines represent the error (standard deviation) due to uncertainty of onset and end dates (see section 3.1).

Using a 7-day moving average of MPE values we found that the precision, sensitivity, specificity and accuracy of a test to detect a lava extrusion phase vary depending on the threshold (Fig. 7): the precision increases with higher thresholds, but the sensitivity decreases, which means that it's more likely to miss events. The optimal threshold value to detect lava extrusion is one that maximizes the precision and accuracy, while keeping the sensitivity and specificity high. In Section 3.2 we found that the 20 MJ MPE value marks a change in trends between the probabilities (Fig.5). Using this same value as a threshold, the test to detect lava extrusion phases has an accuracy = 0.90 +/-0.02, a precision= 0.73+/-0.02, a specificity = 0.96 +/- 0.01, and a sensitivity = 0.56 +/- 0.01. In other words, the model is correct ~ 90% of days (accuracy); approximately 73% of days with MPE>=20MJ had lava extrusion (precision), approximately 96% of days were correctly classified as days with no lava (specificity), and about 56% of the days when lava extrusion occurred had also MPE >= 20MJ (sensitivity).

Our analysis allow us to calculate the conditional probability to detect a lava extrusion phase as a function of the MPE intervals using Eqs.(1,2), but also the conditional probabilities as a function of MPE thresholds Eqs.(5-8). In principle, both approaches can be used for evaluating the probability to observe an on-going lava extrusion phase for any purpose. The MPE time series can be converted directly to the probability to observe a lava extrusion phase ($P(I|k)$, Fig.8 a), and (or) an energy threshold could be used to set different alert levels based on the values of the various probabilities (Fig 8 b).
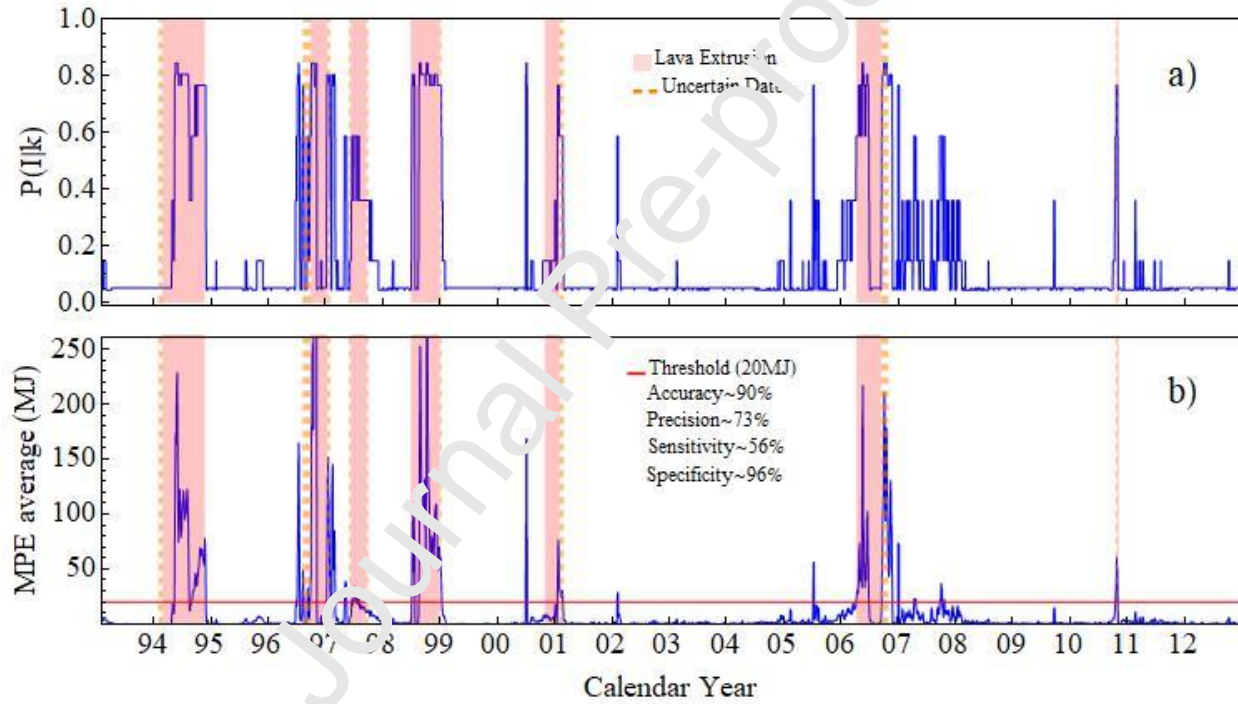
Figure 8. a) Probability to detect a lava extrusion phase $P(I|k)$, Eq.(2), using a 7-day moving average. The probability was calculated using the whole time series from 1993-2012. b) Past 7-day moving average of MPE. The red line a threshold of 20MJ which gives the values of the probabilities of lava extrusion as reported inside the panel. The light-red vertical bands are periods of reported lava extrusion and the uncertainties on the dates are represented by vertical dashed red lines.

3.3. Application to the 2018 Merapi unrest

We further tested our method on Merapi's lava extrusion event of 2018 (Fig.9a) and illustrate how the probability to detect a lava extrusion phase obtained from the previous calculations can be used in real time (Fig.9c). We also compare the effectiveness of the value of 20MJ as a threshold by calculating Eqs.(5-8) for 2018 (Fig.9b). The visual camera installed by CVGHM at the crater captured the beginning of the lava dome formation on 11 August 2018.

We find that for the 2018 dataset the (past) 7-day moving average of MPE continuously exceeded the 20 MJ threshold 14 days early than the observed onset of lava extrusion; overall for this threshold the test has an accuracy=79%, precision =67%, sensitivity = 92%, and specificity = 70%, here we don't have associated uncertainties as in Fig.7 because for 2018 there is an accurate register of the dates when the lava extrusion phase took place.
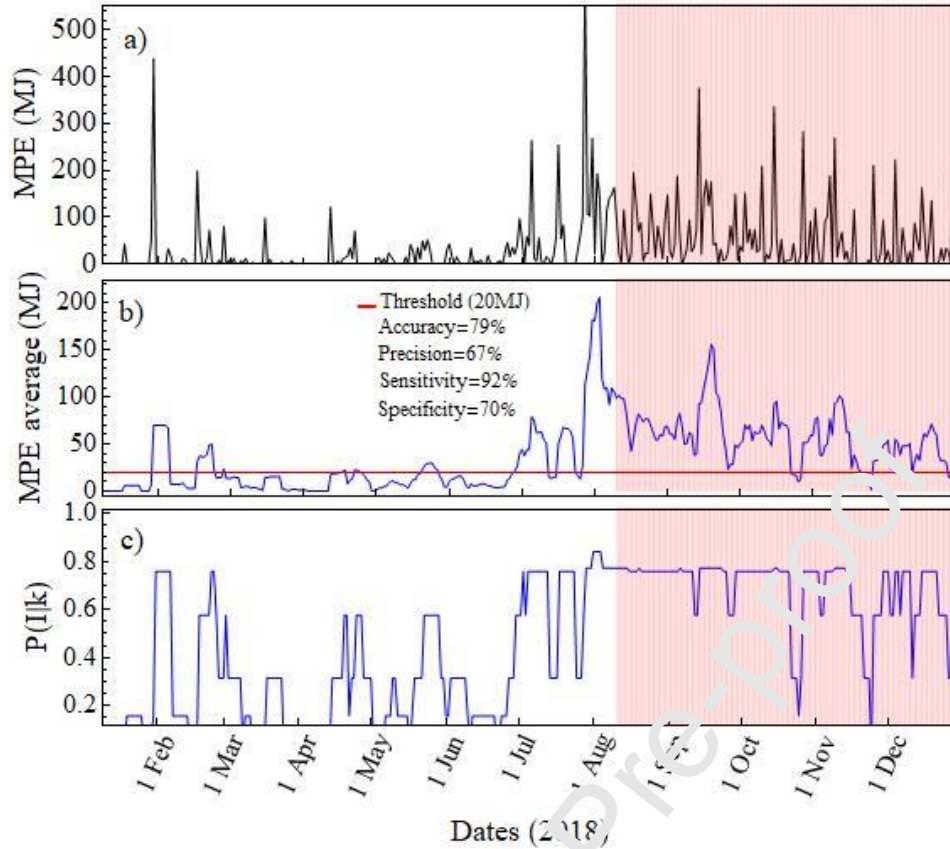
Figure 9. a) Merapi daily MPE from Jan-Dec 2018. The red area indicates the period when dome extrusion was reported. b) the (Past 7-day) moving average of the MPE with a threshold of 20 MJ and the corresponding values of the probability highlighted inside the panel. c). Probability to have lava extrusion Eq.(2), using the probabilities from 1993-2012.

3.4 Probability of occurrence of pyroclastic flows

The lava extrusion phases at Merapi are particularly important because they are dome building, and the eventual dome collapse leads to RFs and PFs, which are among the most hazardous phenomena of Merapi (Voight et al., 2000; Surono et al., 2012). Many variables control the dome collapse e.g. its morphology, the extrusion rate, the slope instability. Young (2007) investigated the relation between major dome-collapse events and extrusion rates and found that most major dome collapse occurred during periods of elevated extrusion rate (>15,000 m3/day or > 0.17 m3/s), which was often preceded by intensifying MP earthquake activity among other

parameters. Iguchi et al. (2019) found a log-log linear correlation between the cumulative seismic energy and the PF flow volume.
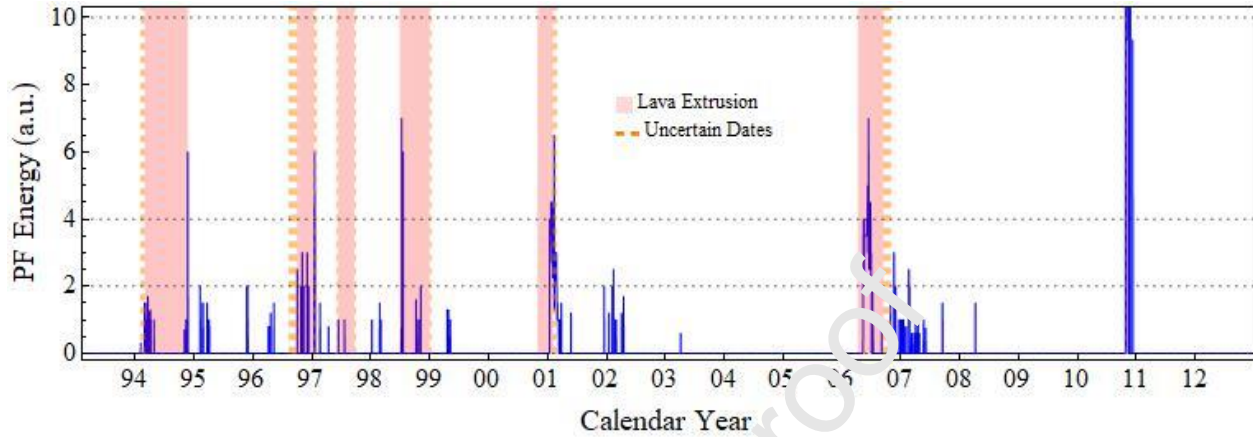

Fig.10. PF energy time series (in a.u.= arbitrary units) between 4 February 1993 to 31 December 2012 in blue bars. The light-red vertical bands mark the lava extrusion phases, the uncertainties in the dates are shown as vertical dashed red lines.

We also analyzed the PF seismic energy originated by the dome collapses from 1993 to 2012 (Fig. 10). As described in section 2.1, the PF seismic signals have a more impulsive onset of long duration and large enough amplitudes to be registered at the farthest seismic stations (e.g. Fig. 1b). As expected, we found that there is an increase of PF activity during lava extrusion phases (Fig.10). Moreover, we found that ~ 86% of the largest (>4 a.u) PFs up to the 2010 event occurred when MPE > 20MJ, which is consistent with Young's (2007) findings that PFs occur more often during periods of dome growth. The PF events that occurred after the onset of the lava-dome growth in 2010 are a different case, as they released > 100 x energy than all the PFs of the previous 17 years, although the MPE incorrectly seems low because the seismic signal from short period instruments (including PUS station) were saturated by LF events (Budi-Santoso et al., 2013). As noted by Surono et al., (2012) and Pallister et al., (2013), the lava

extrusion rate during the 2010 eruption was anomalously large ~25-35 m^3/s, much larger than the

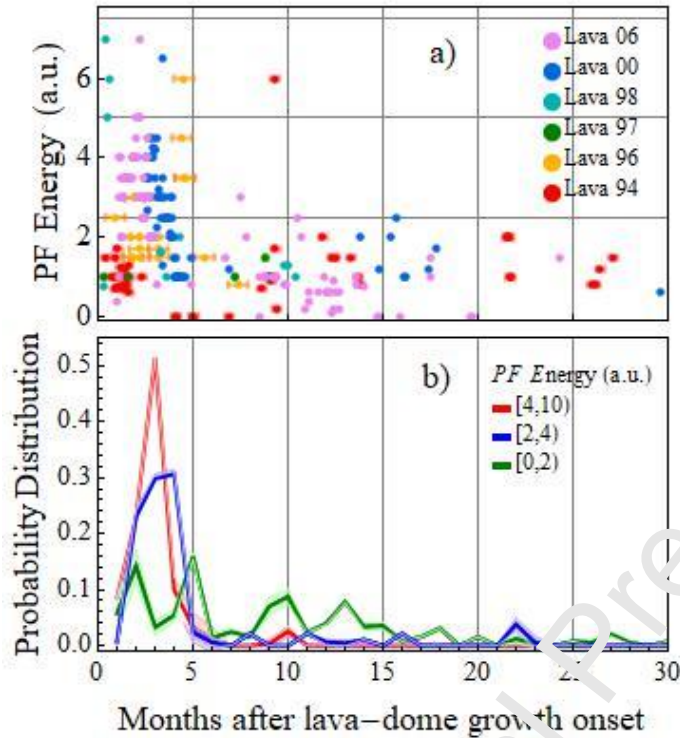Merapi average extrusion rate ~0.1 m^3/s (Young, 2007).

Fig.11 a) PF energy as a function of the time of occurrence with respect to the last lava extrusion onset. The PF that happened between the onset of 1994 and 1996 is labeled lava 94, and analogously for the rest. b) Probability Distribution for PF energy for different ranges as a function of the time of occurrence respect to the lava extrusion phase onset.

We also evaluated whether there is a time correlation between the peak occurrences of PFs, and

the lava extrusion phases onset. We found that the most energetic and thus potentially dangerous

PFs occurred within the first months after the lava extrusion phase onset (Fig. 11). The only case

that differs from this pattern is the PF of 1994, when a large PF of $\sim 6x10^8 \, a.u$, happened 9

months after the lava extrusion phase onset (Ratdomopurbo & Poupinet, 2000). As noted above,

the 2010 event was different, with explosions starting within days of the lava extrusion phase

(Fig. 12), and thus the processes that lead to the explosion and PFs were very different from

previous ones (Surono et al., 2012; Budi-Santoso et al., 2013 and Cronin et al., 2013).
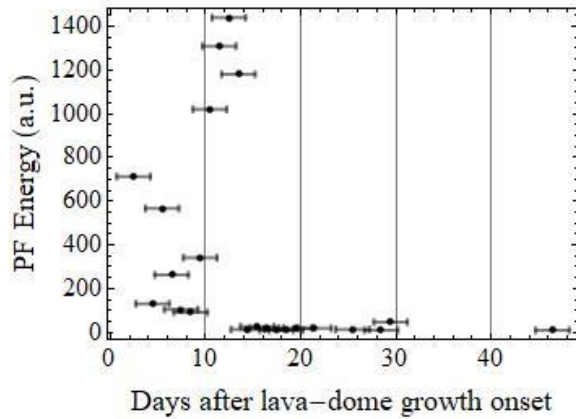
Fig.12. PF energy as a function of the time of occurrence after the 2010's lava-dome growth onset

.

In summary, we found that for the first 6 lava extrusion phases before 2010, the majority of the most energetic PF activity happened within the first 3 months after the onset of the lava extrusion: 83% of PF energy in the range $[4,10)$ x 10^8 a.u. and $53 \pm 3\%$ in the range $[2,4)$ $x10^8$ a.u.. The PF of 2010 occurred much within the same period but much faster (Fig 12).

4.Discussion

Our manuscript aims at contributing to develop methodologies for the correct identification and detection of different eruptive phases and their associated hazards. To achieve this it is essential to have long time series of monitoring data that are self-consistent and standardized (e.g. WOVOdat; Newhall et al., 2017), identify patterns or structures within the data which may be diagnostic of the various types of activities, and have modeling or a statistical tool that can translate the data into useful or applicable results to mitigate the hazards. These three aspects and possible applications of our method to other volcanoes are discussed in turn below.

4.1 Data standardization and uncertainties

An important aspect to successfully detect an eruptive phase is to have enough data that are curated and standardized in a manner that can be aggregated for statistical analysis. In our case, we have 7 lava extrusion phases comprising 3 total accumulated years of extrusive activity over an observation window of 19 years. During this time, the CVGHM closely monitored Merapi volcano and developed a systematic method to manually classify the seismic events. However, due to the active nature of the volcano and the changes in the technology over time, there are some inconsistencies in the monitoring data and the records of volcanic activity. For example, during the 2010 eruption, there was a disruption on the monitoring network; the intensified LF seismic events produced amplitude saturation of the PUS short period instrument (Budi-Santoso et al., 2013) overshadowing other earthquake types like the MP. Later on 4 November, the PUS and DEL stations were destroyed and subsequently the seismic activity was registered only using the PLA station.

Another source of uncertainty in our dataset is the lack of accurate dates when lava extrusion phases occurred, as most observations were via direct visual inspection of the volcano's summit which (due the occurrence of PF currents and explosions) carried major risks. Only recently, the monitoring network acquired thermal high-resolution visual images and movies in stereoscopic configurations (Kelfoun et al., 2021). Also, unmanned aerial vehicles (UAV) and satellite remote sensing analysis using Synthetic Aperture Radar (SAR) was used to detect morphological changes as well as to quantify lava-dome extrusion rates during the 2006 and 2010 eruptions (Pallister et al., 2013; Walter et al., 2013; Darmawan et al., 2018).

We were able to take into account the uncertainty of the chronologies of lava extrusion phases by using Monte Carlo simulations that randomly select different scenarios for the duration of the lava extrusion phases and perform a statistical analysis for each case. In contrast to other stochastic approaches that aim to forecast the sequence of eruptive events or the distribution of eruptive phases by calculating the probability of transition between different states (Bebbington & Lai, 1996; Marzocchi & Zaccarelli, 2006; Bebbington, 2008; Bebbington & Jenkins, 2019), here we focus simply on the calculation of the probabilities to observe lava extrusion phase (dome formation) as a function of the MPE levels. Notwithstanding the simplified approach we have used, we still find clear trends linking lava extrusion with the MPE levels and their time evolution. The identification of these trends (Figs.5,6,7) is possible thanks to the exceptionally long time series analyzed that allowed us to have 7270 days (1993-2012) of representative sampling data, highlighting the importance of long-term analysis.

4.2 Ambiguous interpretation of seismic activity

We found that the values of the calculated probabilities reflect a strong correlation between the MPE levels and lava extrusion phases, however this relation is not reciprocally conditional at Merapi. For example, there were several periods when dome formation was observed but the MPE values were null or minimal. In 1994, the onset of the lava extrusion phase was reported in February but the daily MPE was null until the end of April (Ratdomopurbo & Poupinet, 2000). Again, at the end of October 2000, a new lava extrusion phase was observed (Table 4 & supplementary material), but the MPE level was minimal until it increased in early January and came along with a large PF event. Finally, in 2006 there was a gap between July and mid-September, when the MPE values were very low although dome formation was reported

(Ratdomopurbo et al., 2013). In contrast, there were periods between 2001-2006 and 2007-2008 where the MPE activity exceed the 20MJ (and therefore the probability to have lava extrusion >0.5), but there was no dome formation reported. Moreover, the MP seismic events can be related to several physical phenomena, such as fractures and faulting in the volcanic conduit associated with magma ascent, pressurization (Harrington, R. M., & Brodsky, E. E. 2007) or release of gas and ash between cracks (Neuberg et al., 2006).

Given these observations and those in other volcanic systems, the relation between the effusion rates and the MP seismicity is likely nonlinear. Low values of MPE or a gap in seismicity during lava extrusion phases can be attributed to slow extrusion rate (Carr et al. (2016)), or exogenous dome growth through an open feeder conduit (which can take place during very high extrusion rate periods), and therefore it can occur without the prevalent brittle failure mechanism (Lamb et al. (2014)). Perhaps, if the lava extrusion rates can be determined with higher accuracy (Kelfoun et al. (2021); Pallister et al. (2013); Walter et al. (2013); Darmawan et al. (2018)), it might be possible to interpolate the relation between the MPE levels and the extrusion rate if these time series are compared during a long enough period of time.

Notwithstanding these complexities, the high value of the probabilities calculated reflect a strong correlation between the levels of MPE and lava extrusion phases. In the particular case of the 2018's lava extrusion phase, the MPE levels indicated an on-going lava extrusion phase 14 days before it was detected by the visual camera. Similar process can be expected at other volcanoes but since the volcanic systems may differ, they would need further studies.

4.3 Simplifications and the use of thresholds

The analysis of monitoring data to calculate probability we report is simpler than other studies, as it does not use the time sequence of seismicity (Boué et al., 2015, Jaquet et. al., 2006, Bell & Kilburn, 2013, Carlà et. al. 2016). We also performed a cursory analysis of the time sequence length and size of MPE before the eruptive phases, but we did not find systematic patterns, and thus we decided to simplify and use threshold of seismicity which can also be successfully employed to make decisions at volcano observatories (e.g. Potter et al. 2015). Moreover, we focus only on lava extrusion phases because they produce hazardous PFs and show an apparently simple seismic signature, although other important types of eruptive activity also occur at Merapi (vulcanian explosions, lateral blasts, or phreatic explosions: Young 2007; Surono et al., 2012; Ratdomopurbo et. al., 2013; Budi-Santoso et al., 2018b; Metaxian et al., 2020).

Despite the simplicity of our analysis, we are able to identify the relevant seismic energy range that characterizes lava extrusion. This allows to address questions such as what is the probability that lava is extruding given an observed daily MPE? Moreover, continued analysis of future eruption data should improve the performance of the method and allow the refinement of the threshold values that could be used operationally to make decisions to mitigate volcano hazards impacts (Potter et.al. 2015). We found that the relevant threshold has increased for recent years (Fig.6), mostly due to the high MPE that marked the inter-eruption period between the end of 2006 and the onset of the 2010 lava dome extrusion that was associated with a higher explosivity (Surono et al., 2012). The change in the energy threshold may relate to shifts in the volcanic behavior associated with possible obstruction of the volcanic conduits due to old domes. In fact, we observed a long period without lava extrusion phases between 2001 and 2006, as well as between 2006 to 2010, that msy explain this shift in the energy threshold.

Although the MPE can be used to identify on-going lava extrusion with high precision and accuracy (Figs.8,9), it has a limited use as a forecasting tool. The MPE of the precursory period (II) overlaps with both the active period (I) and the non-active period (III), making it difficult to differentiate one from another using simple energy thresholds. Moreover, the absence of significant MP seismicity preceding the lava extrusion phases for some years (1994 and 2000) and the long unrest periods for others (2006), did not allow the identification of a precursory period with similar duration for all the lava extrusion phases. Finally, the MP earthquakes are mostly at shallow depths (Budi-Santoso et al., 2013; Ratdomopurbo & Poupinet, 2000), thus, they appear more often when the lava extrusion is already on-going. Volcanic activity involves many different types of earthquakes (e.g. Ratdomopurbo & Poupinet, 2000; White & McCausland, 2016; Arambula-Mendoza et al., 2018) and other monitoring data (Potter et. al., 2015) that we have not used, and hence our model could be improved by making a multiparametric analysis that combines probabilities from different monitoring data indicators.

Finally, we also analyzed the relation between the lava extrusion and the PF events and found that 83% of the dome collapse PFs occurred within the first 3 months of lava extrusion phases. The MPE thresholds and the time after the start of the lava extrusion phase can be used by volcano observatories as a guide for the likelihood that dome eruption is occurring at the summit and thus characterize the possibility of pyroclastic flows to occur.

4.4 Possible applications to other volcanoes

A similar approach to the one we have presented here could be applied to other volcanoes and quantitatively correlate monitoring data to eruptive phases. This would require the gathering of

statistically significant data of daily sampling rate for eruptive phases of long duration (e.g. lava flow, shallow magma intrusion/cryptodome, continuous ash emission) such as the one we have studied, but events or eruptive phases of shorter duration (e.g. explosion, ash venting), would require higher sampling rate data.

Example of volcanoes with intermittent long-duration eruption phases, such as those that grow viscous domes, are Redoubt (Miller, 1994), Soufrière Hills (Miller et al., 1998; Lamb et al., 2014), Unzen (Nakada et al., 1999; Shi et al., 2018), St. Helens (Salzer et al., 2016), Santiaguito (Anderson et al., 1995), Sinabung (Gunawan et al., 2019) and Volcán de Colima (Robin et al., 1991; Lamb et al., 2014; Arámbula-Mendoza et al., 2019). This methodology could be applied to other eruptive phase types besides lava extrusion, such as intermittent ash emission like at Popocatepetl (Alvarez-Ramirez et al. (2009)), and stalled magmatic intrusion or failed eruption (Moran and Roman, 2011) such as at Souhière Guadeloupe (Feuillard et al., 1983), Akutan (Lu et al., 2000), Iliamna (Roman et al., 2004; Roman and Power, 2011), Iwate (Nishimura and Ueki, 2011), Paricutin (Gardine and Cox, 2011) and Kilauea (Bell and Kilburn, 2013).

Our approach could be useful especially for volcanoes where direct observation and field mapping are not possible due to the level of hazard or are difficult to observe (e.g. inner crater lava flows), such as at Shinmoe-dake (Kato and Yamasato, 2013); Agung (Syahbana et al., 2019); and Ruang (Kaneko et al., 2019). To detect short-duration eruptive phase or events (e.g. explosion, ash venting Cole et al., 2014) would require a higher sampling rate data, e.g. acoustic infrasound, realtime seismic amplitude measurement (RSAM) and displacement seismic amplitude ratio (DSAR).This general method and the processed data we have used are available in WOVOdat (https://dome.wovodat.org/probability/).

5. Conclusions

We have developed a simple but general probabilistic approach to correlate monitoring time series with a specific volcanic activity (eruption phase) accounting for uncertainties in the historical records with Monte Carlo simulations. We used the daily values of MPE seismicity from 4 February 1993 to 31 December 2012, to characterize lava extrusion phases that lead to dome formation at Merapi. We calculated the conditional probability that lava extrusion was occurring as a function of the daily MPE, and found an MPE threshold that indicates lava extrusion with a 90% accuracy. We also characterized the PF activity and found that, the most energetic PFs occurred during high lava extrusion and that 83% happened within the first 3 months of lava extrusion. The methodology that we have used could be implemented at volcano observatories to compare a given episode of unrest with the historical data. Our method allows for more quantitative assessment of hazards during volcanic crises and thus may help to mitigate the impacts of volcanic activity.

CVGHM in "Assessment and Mitigation of Geological Hazards". Kasbani, Hanik Humaida, Hendra Gunawan, I.G.M. Nandaka from CVGHM are thanked for their support. We also would like to thank Mr. Nguyen Tien Nhan and Mr. Nguyen To Vinh Huy for their help in the development of the WOVOdat analytics tool interface. The authors wish to acknowledge of many other colleagues at BPPTKG-CVGHM for their contribution in various ways. We would also like to thank the reviewers for their insightful reviews.

Appendix A

The seismic data used for our calculations can be found online at:

https://wovodat.org/about/MerapiAnalyticPaper2022.php

References

Aisyah, N., Iguchi, M., Subandriyo, Budisantoso, A., Hotta, K., Sumarti, S., 2018. Combination of a pressure source and block movement for ground deformation analysis at merapi volcano prior to the eruptions in 2006 and 2010. Journal of Volcanology and Geothermal Research 357, 239–253. doi:https://doi.org/10.1016/j.jvolgeores.2018.05.001

Alvarez-Ramirez, J., Sosa, E., & Rodriguez, E. (2009). Assessing temporal-dependent correlations in the 2000–2008 Popocatepetl exhalation sequence by using detrended fluctuation analysis. *Journal of Volcanology and Geothermal Research*, *186*(3–4), 426–431. https://doi.org/10.1016/j.jvolgeores.2009.05.022

Anderson, S.W., Fink, J.H., Rose, W.I., 1995. Mount St. Helens and Santiaguito lava domes: The effect of short-termeruption rate on surface texture and degassing processes. Journal of Volcanology and Geothermal Research 69, 105 – 116. doi:https://doi.org/10.1016/0377-0273(95) 00022-4.

Arámbula-Mendoza, R., Reyes-Dávila, G., Vargas-Bracamontes Dulce, M., González-Amezcua, M., Navarro-Ochoa, C., Martínez-Fierros, A., Ramírez-Vázquez, A., 2018. Seismic monitoring of effusive-explosive activity and large lava dome collapses during 2013–2015 at Volcán de Colima, Mexico. Journal of Volcanology and Geothermal Research 351, 75 – 88. doi:https://doi.org/10.1016/j.jvolgeores.2017.12.017.

Arnold, D.W.D., Biggs, J., Anderson, K., Vallejo Vargas, S., Wadge, G., Ebmeier, S.K., Naranjo, M.F., Mothes, P., 2017. Decaying Lava Extrusion Rate at El Reventador Volcano, Ecuador, Measured Using High- Resolution Satellite Radar. Journal of Geophysical Research: Solid Earth 122, 9966–9988. doi:https://doi.org/10.1002/2017JB014580.

Beauducel, F., Agung Nandaka, M., Cornet, F., Diament, M., 2006. Mechanical discontinuities monitoring at Merapi volcano using kinematic GPS. Journal of Volcanology and Geothermal

Research 150, 300–312. doi:https://doi.org/10.1016/j.jvolgeores.2005.07.005.

Beauducel, F., Cornet, F.-H., Suhanto, E., Duquesnoy, T., & Kasser, M. (2000). Constraints on magma flux from displacements data at Merapi volcano, Java, Indonesia. *Journal of Geophysical Research: Solid Earth*, *105*(B4), 8193–8203. https://doi.org/10.1029/1999JB900368

Bebbington, M. (2008). Incorporating the eruptive history in a stochastic model for volcanic eruptions. *Journal of Volcanology and Geothermal Research*, *175*(3), 325–333. https://doi.org/10.1016/j.jvolgeores.2008.03.013

Bebbington, M. S., & Lai, C. D. (1996). Statistical analysis of New Zealand volcanic occurrence data. *Journal of Volcanology and Geothermal Research*. https://doi.org/10.1016/S0377-0273(96)00050-9

Bebbington, Mark S., & Jenkins, S. F. (2019). Intra-eruption forecasting. *Bulletin of Volcanology*, *81*(6), 34. https://doi.org/10.1007/s00445-019-1294-9

Bell, A. F., & Kilburn, C. R. J. (2013). Trends in the aggregated rate of pre-eruptive volcano-tectonic seismicity at Kilauea volcano, Hawaii. *Bulletin of Volcanology*, *75*(1), 677. https://doi.org/10.1007/s00445-012-0677-y

Boué, A., Lesage, P., Cortés, G., Valette, B., & Reyes-Dávila, G. (2015). Real-time eruption forecasting using the material Failure Forecast Method with a Bayesian approach. *Journal of Geophysical Research: Solid Earth*, *120*(4), 2143–2161. https://doi.org/10.1002/2014JB011637

Brodscholl, A., Kirbani, S., Voight, B., 2000. Sequential dome collapse nuées ardentes analyzed from broadband seismic data, Merapi Volcano, Indonesia. Journal of Volcanology and Geothermal Research 100, 363–369. doi:https://doi.org/10.1016/S0377-0273(00)00145-1.

Budi-Santoso, Agus; Subandriyo; Humaida, Harli; Senarto; Suparwoko, H. . M. Y. B. S., & Amto. (2008). Perkembangan dan Morfologi Kubah Lava Merapi (2006) Berdasarkan Data Analisis Visual. *Laporan BPPTKG, CVGHM, Geological Agency*, 55–78.

Budi-Santoso, A., Lesage, P., Dwiyono, S.. Semarti, S., Subandriyo, Surono, Jousset, P., & Metaxian, J.-P. (2013). Analysis of the seismic activity associated with the 2010 eruption of Merapi Volcano, Java. *Journal of Volcanology and Geothermal Research*, *261*, 153–170. https://doi.org/https://doi.org/10.1016/j.jvolgeores.2013.03.024

Budi-Santoso, A., Rudianto, I., Widyblaksono, R., Sulistiyani, Fajiculay, E., Win, N., Widiwijayanti, C., Costa, F., 2018b. Fuzzy inference system for merapi alert level decision making, in: Abstract volume of the international meeting Cities on Volcanoes (CoV) 10, Miscellanea INGV No. 43. ISSN 2039-6651, p. 54.

Bull, K.F., Buurman, H., 2013. An overview of the 2009 eruption of Redoubt Volcano, Alaska. Journal of Volcanology and Geothermal Research 259, 2–15. doi:https://doi.org/10.1016/j.jvolgeores.2012. 06.024. the 2009 Eruption of Redoubt Volcano, Alaska.

Calder, E. S., Luckett, R., Sparks, R. S. J., & Voight, B. (2002). Mechanisms of lava dome instability and generation of rockfalls and pyroclastic flows at Soufrière Hills Volcano, Montserrat. *Geological Society, London, Memoirs*, *21*(1), 173–190. https://doi.org/10.1144/GSL.MEM.2002.021.01.08

Calder, Eliza S., Lavallée, Y., Kendrick, J. E., & Bernstein, M. (2015). Lava Dome Eruptions. In *The Encyclopedia of Volcanoes* (pp. 343–362). Elsevier. https://doi.org/10.1016/B978-0-12-385938-9.00018-3

Carlà, T., Intrieri, E., Di Traglia, F., & Casagli, N. (2016). A statistical-based approach for determining the intensity of unrest phases at Stromboli volcano (Southern Italy) using one-step-ahead forecasts of displacement time series. *Natural Hazards*, *84*(1), 669–683. https://doi.org/10.1007/s11069-016-2451-5

Carn, S. ., Watts, R. ., Thompson, G., & Norton, G. . (2004). Anatomy of a lava dome collapse: the 20 March 2000 event at Soufrière Hills Volcano, Montserrat. *Journal of Volcanology and Geothermal Research*, *131*(3–4), 241–264. https://doi.org/10.1016/S0377-0273(03)00364-0

Carr, B. B., Clarke, A. B., & Vanderkluysen, L. (2016). The 2006 lava dome eruption of Merapi Volcano (Indonesia): Detailed analysis using MODIS TIR. *Journal of Volcanology and Geothermal Research*, *311*, 60–71. https://doi.org/https://doi.org/10.1016/j.jvolgeores.2015.12.004

Cashman, K.V., Sparks, R.S.J., 2013. How volcanoes work: A 25 year perspective. GSA Bulletin 125, 664–690. doi:10.1130/B30720.1.

Cole, P.D., Smith, P.,Komorowski, J.C., Alfano, F., Bonadonna, C., Stinton, A., Christopher, T., Odbert, H.M., Loughlin, S., 2014. Ash venting occurring both prior to and during lava extrusion at Soufrière Hills Volcano, Montserrat, from 2005 to 2010, in: The Eruption of Soufrière Hills Volcano, Montserrat from 2000 to 2010. Geological Society of London. doi:10.1144/M39.4.

Coppola, D., Laiolo, M., Cigolini, C., Donne, D.D., Ripepe, M., 2016. Enhanced volcanic hot-spot detection using MODIS IR data: results from the MIROVA system, in: Detecting, Modelling and Responding to Effusive Eruptions. Geological Society of London. doi:10.1144/SP426.5.

Costa, F., Widiwijayanti, C., Nang, T. Z. W., Fajiculay, E., Espinosa-Ortega, T., & Newhall, C. (2019). WOVOdat – the global volcano unrest database aimed at improving eruption forecasts. *Disaster Prevention and Management: An International Journal*, *28*(6), 738–751. https://doi.org/10.1108/DPM-09-2019-0301

Cronin, S. J., Lube, G., Dayudi, D. S., Sumarti, S., Subrandiyo, S., & Surono. (2013). Insights into the October–November 2010 Gunung Merapi eruption (Central Java, Indonesia) from the stratigraphy, volume and characteristics of its pyroclastic deposits. *Journal of Volcanology and Geothermal Research*, *261*, 244–259. https://doi.org/https://doi.org/10.1016/j.jvolgeores.2013.01.005

Darmawan, H.,Walter, T.R., Brotopuspito, K.S., Subandriyo, I Gusti Made Agung Nandaka, 2018. Morphological and structural changes at the Merapi lava dome monitored in 2012–15 using unmanned aerial vehicles (UAVs). Journal of Volcanology and Geothermal Research 349, 256– 267. doi:https://doi.org/10.1016/j.jvolgeores.2017.11.006.

De Angelis, S., Bass, V., Hards, V., & Ryan, G. (2007). Seismic characterization of pyroclastic flow activity at Soufrière Hills Volcano, Montserrat, 8 January 2007. *Natural Hazards and Earth System Sciences*, *7*(4), 467–472. https://doi.org/10.5194/nhess-7-467-2007

Fawcett, T., 2006. An Introduction to ROC Analysis. Pattern Recogn. Lett. 27, 861–874. doi:10.1016/j.patrec.2005.10.010.

Feuillard, M., Allegre, C., Brandeis, G., Gaulon, R., Le Mouel, J., Mercier, J., Pozzi, J., Semet, M., 1983. The 1975–1977 crisis of la Soufriere de Guadeloupe (F.W.I): A still-born magmatic eruption. Journal of Volcanology and Geothermal Research 16, 317–334. doi:https://doi. org/10.1016/0377-0273(83)90036-7.

Flower, V.J., Carn, S.A., 2015. Characterising volcanic cycles at Soufriere Hills Volcano, Montserrat: Time series analysis of multi-parameter satellite data. Journal of Volcanology and Geothermal Research 304, 82–93. doi:https://doi.org/10.1016/j.jvolgeores.2015.07.035.

Gardine, M., W.M., Cox, T., 2011. Dike emplacement near Parícutin volcano, Mexico in 2006. Bull Volcanol 73, 123–132. doi:https: //doi.org/10.1007/s00445-010-0437-9.Gardner, C. A., & White, R. A. (2002). Seismicity, gas emission and deformation from 18 July to 25 September 1995 during the initial phreatic phase of the eruption of Soufrière Hills Volcano, Montserrat. *Geological Society,*

London, Memoirs, *21*(1), 567–581. https://doi.org/10.1144/GSL.MEM.2002.021.01.26

Gardner, C.A., White, R.A., 2002. Seismicity, gas emission and deformation from 18 July to 25 September 1995 during the initial phreatic phase of the eruption of Soufrière Hills Volcano, Montserrat. Geological Society, London, Memoirs 21, 567–581. doi:10.1144/GSL.MEM.2002.021.01.26.

Gerstenecker, C., Läufer, G., Steineck, D., Tiede, C., Wrobel, B., 2005. Validation of Digital Elevation Models around Merapi Volcano, Java, Indonesia. Natural Hazards and Earth System Sciences 5, 863–876. doi:10.5194/nhess-5-863-2005.

Global Volcanism Program, 2013. Merapi (263250) in Volcanoes of the World, v. 4.10.3 (15 Oct 2021). doi:https://doi.org/10.5479/si.GVP. VOTW4-2013.

Gottsmann, J., Neuberg, J., & Scheu, B. (2019). Volcanic Unrest. In J. Gottsmann, J. Neuberg, & B. Scheu (Eds.), *Advances in Volcanology*. Springer International Publishing. https://doi.org/10.1007/978-3-319-58412-6

Gunawan, H., Surono, Budianto, A., Kristianto, Prambada, O., McCausland, W., Pallister, J., Iguchi, M., 2019. Overview of the eruptions of sinabung volcano, 2010 and 2013–present and details of the 2013 phreatomagmatic phase. Journal of Volcanology and Geothermal Research 382, 103–119. doi:https://doi.org/10.1016/j.jvolgeores.2017. 08.005.

Gutenberg, B., & Richter, C. F. (1956). Earthquake magnitude, intensity, energy, and acceleration: (Second paper). *Bulletin of the Seismological Society of America*.

Hale, A. J. (2008). Lava dome growth and evolution with an independently deformable talus. *Geophysical Journal International*, *174*(1), 391–417. https://doi.org/10.1111/j.1365-246X.2008.03806.x

Harrington, R. M., & Brodsky, E. E. (2007). Volcanic hybrid earthquakes that are brittle-failure events. *Geophysical Research Letters*, *34*(6), L06308 https://doi.org/10.1029/2006GL028714

Heap, M. J., Troll, V. R., Kushnir, A. R. L., Gilg, H. A., Collinson, A. S. D., Deegan, F. M., Darmawan, H., Seraphine, N., Neuberg, J., & Walter, T. R. (2019). Hydrothermal alteration of andesitic lava domes can lead to explosive volcanic behaviour. *Nature Communications*, *10*(1), 5063. https://doi.org/10.1038/s41467-019-13102-8

Hidayat, D., Chouet, B. A., Voight, B., Dawson, P. B., & Ratdomopurbo, A. (2002). Source mechanism of very-long-period signals accompanying dome growth activity at Merapi Volcano, Indonesia. *Geophysical Research Letters*, *29*(23). http://www.geoscienceworld.org/cgi/georef/georef;2004017756

Hoblitt, R.R., Wolfe, E.W., Scott, W.E., Couchman, M.R., Pallister, J.S., Javier, D., 1996. The preclimactic eruptions of Mount Pinatubo, June 1991. Fire and mud: eruptions and lahars of Mount Pinatubo, Philippines. doi:https://pubs.usgs.gov/pinatubo/.

Iguchi, M., Nakamichi, H., Miyamoto, K., Shimomura, M., Nandaka, I. G. M. A., Budi-Santoso, A., Sulistiyani, & Aisyah, N. (2019). Forecast of the Pyroclastic Volume by Precursory Seismicity of Merapi Volcano. *Journal of Disaster Research*, *14*(1), 51–60. https://doi.org/10.20965/jdr.2019.p0051

Jaquet, O., Carniel, R., Sparks, S., Thompson, G., Namar, R., & Di, M. (2006). *DEVIN : A forecasting approach using stochastic methods applied to the Soufrie ` re Hills Volcano*. *153*, 97–111. https://doi.org/10.1016/j.jvolgeores.2005.08.013

Johnson, J., Lees, J., Gerst, A., Sahagian, D., Varley, N., 2008. Longperiod earthquakes and co-eruptive dome inflation seen with particle image velocimetry. Nature 456, 377–381. doi:https://doi.org/10.1038/ nature07429.

Jousset, P., Budi-Santoso, A., Jolly, A.D., Boichu, M., Surono, Dwiyono, S., Sumarti, S., Hidayati, S., Thierry, P., 2013. Signs of magma ascent in lp and vlp seismic events and link to degassing: An example from the 2010 explosive eruption at merapi volcano, indonesia. Journal of Volcanology and Geothermal Research 261, 171–192. doi:https: //doi.org/10.1016/j.jvolgeores.2013.03.014.

Kaneko, T., Maeno, F., Yasuda, A., 2019. Observation of the eruption sequence and formation process of a temporary lava lake during the June–August 2015 Mt. Raung eruption, Indonesia, using high-resolution and high-frequency satellite image datasets. Journal of Volcanology and Geothermal Research 377, 17–32. doi:https://doi.org/10.1016/j. jvolgeores.2019.03.016.

Kato, K., Yamasato, H., 2013. The 2011 eruptive activity of Shinmoedake volcano, Kirishimayama, Kyushu, Japan—Overview of activity and Volcanic Alert Level of the Japan Meteorological Agency. Earth Planet 65, 2. doi:https://doi.org/10.5047/eps.2013.05.009.

Kelfoun, K., Santoso, A.B., Latchimy, T., Bontemps, M., Nurdien, I., Beauducel, F., Fahmi, A., Putra, R., Dahamna, N., Laurin, A., Rizal M.H., Sukmana, J.T., Gueugneau, V., 2021. Growth and collapse of the 2018–2019 lava dome of Merapi volcano. Bulletin of Volcanology 83, 8. doi:https://doi.org/10.1007/s00445-020-01428-x.Lahr, J. C., Chouet, B. A., Stephens, C. D., Power, J. A., & Page, R. A. (1994). Earthquake classification, location, and error analysis in a volcanic environment: implications for the magmatic system of the 1989–1990 eruptions at redoubt volcano, Alaska. Journal of Volcanology and Geothermal Research, 62(1–4), 137–151. https://doi.org/10.1016/0377-0273(94)90031-0

Lahr, J., Chouet, B., Stephens, C., Power, J., Page, R., 1994. Earthquake classification, location, and error analysis in a volcanic environment: implications for the magmatic system of the 1989–1990 eruptions at redoubt volcano, Alaska. Journal of Volcanology and Geothermal Research 62, 137 – 151. doi:https://doi.org/10.1016/0377-0273(94) 90031-0. the 1989-1990 Eruptions of Redoubt Volcano, Alaska.

Lamb, O.D., De Angelis, S., Umakoshi, K., Hornby, A.J., Kendrick, J.E., Lavallée, Y., 2015. Repetitive fracturing during spine extrusion at Unzen volcano, Japan. Solid Earth 6, 1277–1293. doi:10.5194/se-6-1277-2015.

Lamb, O.D., Varley, N.R., Mather, T.A., Pyle, D.M., Smith, P.J., Liu, E.J., 2014. Multiple timescales of cyclical behaviour observed at two domeforming eruptions. Journal of Volcanology and Geothermal Research 284, 106–121. doi:https://doi.org/10.1016/j.jvolgeores.2014.07.013.

Loughlin, S.C., Sparks, S., Brown, S.K., Jenkins, S.F., Vye-Brown, C., 2015. Global Volcanic Hazards and Risk. Cambridge University Press. doi:10.1017/CBO9781316276273.

Lowenstern, 2016. Abstract volume for the 2016 biennial meeting of the Yellowstone Volcano Observatory: U.S. Geological Survey Open-File Report 2016–1104. doi:http://www.dx.doi.org/10.3133/ofr20161104.

Lu, Z., Wicks Jr., C., Power, J.A., Dzurisin, D., 2000. Ground deformation associated with the March 1996 earthquake swarm at Akutan volcano, Alaska, revealed by satellite radar interferometry. Journal of Geophysical Research: Solid Earth 105, 21483–21495. doi:https://doi.org/10. 1029/2000JB900200.

Luckett, R., Baptie, B., Neuberg, J., 2002. The relationship between degassing and rockfall signals at soufrière hills volcano, montserrat. Geological Society, London, Memoirs 21, 595–602. doi:10.1144/GSL. MEM.2002.021.01.28.

Luckett, R., Loughlin, S., De Angelis, S., Ryan, G., 2008. Volcanic seismicity at montserrat, a comparison between the 2005 dome growth episode and earlier dome growth. Journal of

Volcanology and Geothermal Research 177, 894–902. doi:https://doi.org/10.1016/j.jvolgeores. 2008.07.006. volcanic Flows and Falls.

Marzocchi, W., & Zaccarelli, L. (2006). A quantitative model for the time-size distribution of eruptions. *Journal of Geophysical Research*, *111*(B4), B04204. https://doi.org/10.1029/2005JB003709

McCausland, W. A., Gunawan, H., White, R. A., Indrastuti, N., Patria, C., Suparman, Y., Putra, A., Triastuty, H., & Hendrasto, M. (2019). Using a process-based model of pre-eruptive seismic patterns to forecast evolving eruptive styles at Sinabung Volcano, Indonesia. *Journal of Volcanology and Geothermal Research*, *382*, 253–266. https://doi.org/10.1016/j.jvolgeores.2017.04.004

McNutt, S. R. (2005). VOLCANIC SEISMOLOGY. *Annual Review of Earth and Planetary Sciences*, *33*(1), 461–491. https://doi.org/10.1146/annurev.earth.33.092203.122459

McNutt, S.R., Roman, D.C., 2015. The Encyclopedia of Volcanoes (Second Edition). Second edition ed., Academic Press, Amsterdam. doi:https: //doi.org/10.1016/B978-0-12-385938-9.00059-6.

Melnik, O., & Sparks, R. S. J. (1999). *Nonlinear dynamics of lava dome extrusion*. 37–41.

Miller, A. D., Stewart, R. C., White, R. A., Luckett, R., Baptie, B. J., Aspinall, W. P., Latchman, J. L., Lynch, L. L., & Voight, B. (1998). *Seismicity associated with dome growth and collapse at the Soufriere Hills Volcano , Montserrat. 25*(18), 3401–3404.

Miller, T.P., 1994. Dome growth and destruction during the 1989–1990 eruption of redoubt volcano. Journal of Volcanology and Geothermal Research 62, 197–212. doi:https://doi.org/10.1016/0377-0273(94) 90034-5.

Minakami, T. (1960). Fundamental research for predicting volcanic eruptions (Part I), Earthquakes and crustal deformation originating from volcanic activity. *Bulletin of the Earthquake Research Institute, University of Tokyo*, *38*, 497–544.

Métaxian, J.P., Santoso, A.B., Caudron, C., Cholik, N., Labonne, C., Poiata, N., Beauducel, F., Monteiller, V., Fahmi, A.A., Rizal, M.H., Nandaka, I M.A., 2020. Migration of seismic activity associated with phreatic eruption at Merapi volcano, Indonesia. Journal of Volcanology and Geothermal Research 396, 106795. doi:https://doi.org/10.1016/j. jvolgeores.2020.106795.Nakada, S., Shimizu, H., Ohta, K., 1999. Overview of the 1990–1995 eruption at Unzen Volcano. Journal of Volcanology and Geothermal Research 89, 1–22. doi:https://doi.org/10.1016/S0377-0273(98)00118-8.

Nandaka, I. G. M. A., Sulistiyani, Suharna, Y., & Putra, R. (2019). Overview of Merapi Volcanic Activities from Monitoring Data 1992–2011 Periods. *Journal of Disaster Research*, *14*(1), 18–26. https://doi.org/10.20965/jdr.2019.p0018

Neuberg, J. (2000). Characteristics and causes of shallow seismicity in andesite volcanoes. *Philosophical Transactions of the Royal Society of London. Series A: Mathematical, Physical and Engineering Sciences*, *358*(1770), 1533–1546. https://doi.org/10.1098/rsta.2000.0602

Neuberg, J., Baptie, B., Luckett, R., & Stewart, R. (1998). Results from the Broadband Seismic Network on Montserrat. *Geophysical Research Letters*, *25*(19), 3661–3664. https://doi.org/10.1029/98GL01441

Neuberg, J., Tuffen, H., Collier, L., Green, D., Powell, T., Dingwell, D., 2006. The trigger mechanism of low-frequency earthquakes on Montserrat. Journal of Volcanology and Geothermal Research 153, 37– 50. doi:https://doi.org/10.1016/j.jvolgeores.2005.08.008.

Newhall, C. G., Bronto, S., Alloway, B., Banks, N. G., Bahar, I., del Marmol, M. A., Hadisantono, R. D., Holcomb, R. T., McGeehin, J., Miksic, J. N., Rubin, M., Sayudi, S. D., Sukhyar, R., Andreastuti, S., Tilling, R. I., Torley, R., Trimble, D., & Wirakusumah, A. D. (2000). 10,000Years of explosive eruptions of Merapi Volcano, Central Java: archaeological and modern implications. *Journal of*

Volcanology and Geothermal Research, *100*(1–4), 9–50. https://doi.org/10.1016/S0377-0273(00)00132-3

Newhall, C., Bronto, S., Alloway, B., Banks, N., Bahar, I., del Marmol, M., Hadisantono, R., Holcomb, R., McGeehin, J., Miksic, J., Rubin, M., Sayudi, S., Sukhyar, R., Andreastuti, S., Tilling, R., Torley, R., Trimble, D., Wirakusumah, A., 2000. 10,000Years of explosive eruptions of Merapi Volcano, Central Java: archaeological and modern implications. Journal ofVolcanology and Geothermal Research 100, 9 – 50. doi:https: //doi.org/10.1016/S0377-0273(00)00132-3.

Newhall, C., Costa, F., Ratdomopurbo, A., Venezky, D., Widiwijayanti, C., Win, N.T.Z., Tan, K., Fajiculay, E., 2017. WOVOdat – An online, growing library of worldwide volcanic unrest. Journal of Volcanology and Geothermal Research 345, 184 – 199. doi:https://doi.org/10.1016/j.jvolgeores.2017.08.003.

Newhall, C. G., & Dzurisin, D. (1988). Historical unrest at large calderas of the world. In *US Geological Survey Bulletin*. US Geological Survey. https://pubs.usgs.gov/bul/1855/

Newhall, C. G., & Melson, W. G. (1983). Explosive activity associated with the growth of volcanic domes. *Journal of Volcanology and Geothermal Research*, *17*(1), 111–131. https://doi.org/https://doi.org/10.1016/0377-0273(83)90067-1

Newhall, C., & Hoblitt, R. (2002). Constructing event trees for volcanic crises. *Bulletin of Volcanology*, *64*(1), 3–20. https://doi.org/10.1007/s004450100173

Nishimura, T., Ueki, S., 2011. Seismicity and magma supply rate of the 1998 failed eruption at Iwate volcano, Japan. Bull Volcanol 73, 133– 142. doi:https://doi.org/10.1007/s00445-010-0438-8.Ogburn, S. E., Loughlin, S. C., & Calder, E. S. (2015). The association of lava dome growth with major explosive activity (VEI $\geq$ 4): DomeHaz, a global dataset. *Bulletin of Volcanology*, *77*(5), 40. https://doi.org/10.1007/s00445-015-0919-x

Ogburn, S.E., Loughlin, S.C., S., C.E., 2015. The association of lava dome growth with major explosive activity (VEI $\geq$ 4): DomeHaz, a global dataset. Bulletin of Volcanology 77. doi:https://doi.org/10.1007/ s00445-015-0919-x.

Pallister, J. S., Schneider, D. J., Griswold, J. P., Keeler, R. H., Burton, W. C., Noyles, C., Newhall, C. G., & Ratdomopurbo, A. (2013). Merapi 2010 eruption—Chronology and extrusion rates monitored with satellite radar and used in eruption forecasting. *Journal of Volcanology and Geothermal Research*, *261*, 144–152. https://doi.org/https://doi.org/10.1016/j.jvolgeores.2012.07.012

Pesicek, J. D., Ogburn, S. E., & Prejean, S. G. (2021). Indicators of volcanic eruptions revealed by global M4+ earthquakes. *Journal of Geophysical Research: Solid Earth*, 126, e2020JB021294. https://doi.org/10.1029/2020JB021294

Potter, S. H., Scott, B. J., Jolly, G. E., Neall, V. E., & Johnston, D. M. (2015). Introducing the Volcanic Unrest Index (VUI): a tool to quantify and communicate the intensity of volcanic unrest. *Bulletin of Volcanology*, *77*(9), 77. https://doi.org/10.1007/s00445-015-0957-4

Power, J. A., Lahr, J. C., Page, R. A., Chouet, B. A., Stephens, C. D., Harlow, D. H., Murray, T. L., & Davies, J. N. (1994). Seismic evolution of the 1989–1990 eruption sequence of Redoubt Volcano, Alaska. *Journal of Volcanology and Geothermal Research*, *62*(1–4), 69–94. https://doi.org/10.1016/0377-0273(94)90029-9

Ratdomopurbo, A, & Poupinet, G. (2000). An overview of the seismicity of Merapi Volcano (Java, Indonesia); 1983-1994. *Journal of Volcanology and Geothermal Research*, *100*(1–4), 193–214. http://www.geoscienceworld.org/cgi/georef/georef;2000057503

Ratdomopurbo, Antonius, Beauducel, F., Subandriyo, J., Nandaka, I. G. M. A., Newhall, C. G., Suharna, Sayudi, D. S., Suparwaka, H., & Sunarta. (2013). Overview of the 2006 eruption of Mt. Merapi. *Journal of Volcanology and Geothermal Research*, *261*, 87–97. https://doi.org/https://doi.org/10.1016/j.jvolgeores.2013.03.019

Reath, K., Pritchard, M., Poland, M., Delgado, F., Carn, S., Coppola, D., Andrews, B., Ebmeier, S.K., Rumpf, E., Henderson, S., Baker, S., Lundgren, P., Wright, R., Biggs, J., Lopez, T., Wauthier, C., Moruzzi, S., Alcott, A., Wessels, R., Griswold, J., Ogburn, S., Loughlin, S., Meyer, F., Vaughan, G., Bagnardi, M., 2019. Thermal, Deformation, and Degassing Remote Sensing Time Series (CE 2000–2017) at the 47 most Active Volcanoes in Latin America: Implications for Volcanic Systems. Journal of Geophysical Research: Solid Earth 124, 195–218. doi:https://doi.org/10.1029/2018JB016199.

Robin, C., Camus, G., Gourgaud, A., 1991. Eruptive and magmatic cycles at Fuego de Colima volcano (Mexico). Journal of Volcanology and Geothermal Research 45, 209 – 225.

Roman, D., Neuberg, J., Luckett, R., 2006. Assessing the likelihood of volcanic eruption through analysis of volcanotectonic earthquake fault–plane solutions. Earth and Planetary Science Letters 248, 244–252. doi:https://doi.org/10.1016/j.epsl.2006.05.029.

Roman, D., Power, J., 2011. Mechanism of the 1996–97 noneruptive volcano-tectonic earthquake swarm at Iliamna Volcano, Alaska. Bull Volcanol 73, 143–153. doi:https://doi.org/10.1007/ s00445-010-0439-7.

Roman, D.C., Power, J.A., Moran, S.C., Cashman, K.V., Doukas, M.P., Neal, C.A., Gerlach, T.M., 2004. Evidence for dike emplacement beneath Iliamna Volcano, Alaska in 1996. Journal of Volcanology and Geothermal Research 130, 265–284. doi:https://doi.org/10.1016/ S0377-0273(03)00302-0.

Salzer, J.T., Thelen, W.A., James, M.R., Walter, T.R., Moran, S., Denlinger, R., 2016. Volcano dome dynamics at Mount St. Helens: Deformation and intermittent subsidence monitored by seismicity and camera imagery pixel offsets. Journal of Geophysical Research: Solid Earth 121, 7882–7902. doi:https://doi.org/10.1002/2016JB013045.

Santoso, A.B., Subandriyo, Humaida, H., Sunarto, Suparwoko, H., Miswanto, Yulianto, Badrijas, Suramto, 2008. Perkembangan dan Morfologi Kubah Lava Merapi. Berdasarkan Data Analisis Visual , 55–78.

Segall, P., 2013. Volcano deformation and eruption forecasting, in: Remote Sensing of Volcanoes and Volcanic Processes: Integrating Observation and Modelling. Geological Society of London. doi:10.1144/SP380.4.

Selva, J., Costa, A., Sandri, L., Macedonio, G., & Marzocchi, W. (2014). Probabilistic short-term volcanic hazard in phases of unrest: A case study for tephra fallout. *Journal of Geophysical Research: Solid Earth*, *119*(12), 8805–8826. https://doi.org/10.1002/2014JB011252

Seth C. Moran, C.N., Roman, D.C., 2011. Failed magmatic eruptions: late stage cessation of magma ascent. Bulletin of Volcanology 73, 115–122. doi:https://doi.org/10.1007/s00445-010-0444-x.

Shi, X., Jiang, Y., Hirakawa, Y., 2018. Growth and potential collapse of the lava dome in Unzen volcano and the estimation on block-and-ash flows. Geosciences Journal 22, 273–286. doi:https://doi.org/10.1007/ s12303-017-0051-3.

Shimozuru, D., Miyazaki, T., Gyoda, N., & Matahelumual, J. (1969). Volcanological survey of Indonesian volcanoes; part 2, Seismic observation at Merapi volcano. *Bulletin of the Earthquake Research Institute = Tokyo Daigaku Jishin Kenkyusho Iho*, *47*, *Part 5*, 969–990.

http://www.geoscienceworld.org/cgi/georef/georef;1970018556

Shroder, J. F., & Papale, P. (2015). Volcanic Hazards, Risks and Disasters. In *Volcanic Hazards, Risks, and Disasters*. Elsevier. https://doi.org/10.1016/C2011-0-07012-6

Sparks, R. S. J. (2003). Forecasting volcanic eruptions. *Earth and Planetary Science Letters*, *210*(1–2), 1–15. https://doi.org/10.1016/S0012-821X(03)00124-9

Surono, Jousset, P., Pallister, J., Boichu, M., Buongiorno, M. F., Budisantoso, A., Costa, F., Andreastuti, S., Prata, F., Schneider, D., Clarisse, L., Humaida, H., Sumarti, S., Bignami, C., Griswold, J., Carn, S., Oppenheimer, C., & Lavigne, F. (2012). The 2010 explosive eruption of Java's Merapi volcano—A '100-year' event. *Journal of Volcanology and Geothermal Research*, *241–242*, 121–135. https://doi.org/10.1016/j.jvolgeores.2012.06.018

Syahbana, D., Kasbani, K., Suantika, G., Prambada, O., Andreas, A.S., Saing, U.B., Kunrat, S.L., Andreastuti, S., Martanto, M., Kriswati, E., Suparman, Y., Humaida, H., Ogburn, S., Kelly, P.J., Wellik, J., Wright, H.M.N., Pesicek, J.D.,Wessels, R., Kern, C., Lisowski, M., Diefenbach, A., Poland, M., Beauducel, F., Pallister, J., Vaughan, R.G., Lowenstern, J.B., 2019. The 2017–19 activity at Mount Agung in Bali (Indonesia): Intense unrest, monitoring, crisis response, evacuation, and eruption. Sci Rep 9, 8848. doi:https://doi.org/10.1038/s41598-019-45295-9.

Tonini, R., Sandri, L., Rouwet, D., Caudron, C., Marzocchi, W., & Suparjan. (2016). A new Bayesian Event Tree tool to track and quantify volcanic unrest and its application to Kawah Ijen volcano. *Geochemistry, Geophysics, Geosystems*, *17*(7), 2539–2555. https://doi.org/10.1002/2016GC006327

Umakoshi, K., Takamura, N., Shinzato, N., Uchida, K., Matsuwo, N., Shimizu, H., 2008. Seismicity associated with the 1991-1995 dome growth at Unzen Volcano, Japan. Journal of Volcanology and Geothermal Research 175, 91–99. doi:10.1016/j.jvolgeores.2008.03.030

Voight, B., Constantine, E., Siswowidjoyo, S., Torley, R., 2000a. Historical eruptions of Merapi Volcano, Central Java, Indonesia, 1768–1998. Journal of Volcanology and Geothermal Research 100, 69 – 138. doi:https: //doi.org/10.1016/S0377-0273(00)00134-7.

Voight, B., Young, K. ., Hidayat, D., Subandrio, Purbawinata, M. ., Ratdomopurbo, A., Suharna, Panut, Sayudi, D. ., LaHusen, R., Marso, J., Murray, T. ., Dejean, M., Iguchi, M., & Ishihara, K. (2000). Deformation and seismic precursors to dome-collapse and fountain-collapse nuées ardentes at Merapi Volcano, Java, Indonesia, 1994–1998. *Journal of Volcanology and Geothermal Research*, *100*(1–4), 261–287. https://doi.org/10.1016/S0377-0273(00)00140-2

Walter, T R, Subandriyo, J., Kibkani, S., Bathke, H., Suryanto, W., Aisyah, N., Darmawan, H., Jousset, P., Luehr, B.-G., & Dahm, T. (2015). Volcano-tectonic control of Merapi's lava dome splitting: The November 2013 fracture observed from high resolution TerraSAR-X data. *Tectonophysics*, *639*, 23–33. https://doi.org/https://doi.org/10.1016/j.tecto.2014.11.007

Walter, Thomas R, Ratdomopurbo, A., Subandriyo, Aisyah, N., Brotopuspito, K. S., Salzer, J., & Lühr, B. (2013). Dome growth and coulée spreading controlled by surface morphology, as determined by pixel offsets in photographs of the 2006 Merapi eruption. *Journal of Volcanology and Geothermal Research*, *261*, 121–129. https://doi.org/https://doi.org/10.1016/j.jvolgeores.2013.02.004

Wassermann, J. (2012). Volcano Seismology. In P. Bormann (Ed.), *New Manual of Seismological Observatory Practice (NMSOP-2)*. Deutsches GeoForschungszentrum GFZ; IASPEI. https://doi.org/https://doi.org/10.2312/GFZ.NMSOP-2

Watts, R. B., Herd, R. A., Sparks, R. S. J., & Young, S. R. (2002). Growth patterns and emplacement of the andesitic lava dome at Soufrière Hills Volcano, Montserrat. *Geological Society, London, Memoirs*, *21*(1), 115–152. https://doi.org/10.1144/GSL.MEM.2002.021.01.06

White, R., & McCausland, W. (2016). Volcano-tectonic earthquakes: A new tool for estimating intrusive volumes and forecasting eruptions. *Journal of Volcanology and Geothermal Research*, *309*, 139–155. https://doi.org/10.1016/j.jvolgeores.2015.10.020

Yamasato, H. (1997). Quantitative Analysis of Pyroclastic Flows Using Infrasonic and Seismic Data at Unzen Volcano, Japan. *Journal of Physics of the Earth*, *45*(6), 397–416. https://doi.org/10.4294/jpe1952.45.397

Young, K. D. (2007). Deformation, lava dome evolution, and eruption cyclicity at Merapi volcano, Indonesia. In *ProQuest Dissertations and Theses*. Penn State University.

Zobin, V. (2012). Introduction to Volcanic Seismology. In *Introduction to Volcanic Seismology*. Elsevier. https://doi.org/10.1016/C2011-0-06141-0

Zobin, V.M., Bretón, M., Navarro, C., 2014. Similarity in seismic source scaling relations for tectonic and volcanic processes. Physics of the Earth and Planetary Interiors 231, 65–73. doi:https://doi.org/10.1016/ j.pepi.2014.03.007.

Zorn, E. U., Le Corvec, N., Varley, N. R., Salzer, J. T., Walter, T. R., Navarro-Ochoa, C., Vargas-Bracamontes, D. M., Thiele, S. T., & Arámbula Mendoza, R. (2019). Load Stress Controls on Directional Lava Dome Growth at Volcán de Colima, Mexico. *Frontiers in Earth Science*, *7*. https://doi.org/10.3389/feart.2019.00084

Author statement:

T. Espinosa-Ortega: Conceptualization, Formal Analysis, Writing-Original draft preparation. **A. Budi-Santoso:** Investigation, Data Curation, **Sulistiyani**: Investigation, Data Curation **N-T-Z.Win**: Data Curation, **C.Widiwijayanti**: Conceptualization, Writing- Review & Editing and **F. Costa**: Conceptualization, Writing –Review & Editing, Supervision.

Declaration of interests

☒ The authors declare that they have no known competing financial interests or personal relationships that could have appeared to influence the work reported in this paper.

☐The authors declare the following financial interests/personal relationships which may be considered as potential competing interests:

```



```

- Probabilistic analysis to correlate time series with eruptive phases of long duration.
- Real time detection of dome formation with Daily Hybrid Seismic Energy.
- Mt. Merapi characterization of thresholds for lava extrusion and pyroclastic flow.
- Use of Monte Carlo method to estimate uncertainties due inaccuracy in eruptive phase classification.